Title	Substrate stiffness regulates temporary NF-kappa B activation via actomyosin contractions
Author(s)	Ishihara, Seiichiro; Yasuda, Motoaki; Mizutani, Takeomi; Kawabata, Kazushige; Haga, Hisashi
Citation	Experimental cell research, 319(19), 2916-2927 https://doi.org/10.1016/j.yexcr.2013.09.018
Issue Date	2013-11-15
Doc URL	http://hdl.handle.net/2115/57311
Type	article (author version)
File Information	Ishihara_ECR_2014_final-1.pdf

Instructions for use

1   **Title**: Substrate stiffness regulates temporary NF-κB activation via actomyosin contractions

2

3   Seiichiro Ishihara[a], Motoaki Yasuda[b], Ichiro Harada[c], Takeomi Mizutani[a], Kazushige Kawabata[a],

4   and Hisashi Haga[a, 1]

5

6   [a]Transdisciplinary Life Science Course, Faculty of Advanced Life Science, Hokkaido University,

7   N10-W8, Kita-ku, Sapporo 060-0810, Japan

8   [b]Department of Oral Pathobiological Science, Graduate School of Dental Medicine, Hokkaido

9   University, N13-W7, Kita-ku, Sapporo 060-8586, Japan

10   [c]Department of Biomolecular Engineering, Graduate School of Bioscience and Biotechnology,

11   Tokyo Institute of Technology, 4259 Nagatsuda-cho, Midori-ku, Yokohama 226-8501, Japan

12

13

14   [1]To whom correspondence should be addressed:

15   E-mail: haga@sci.hokudai.ac.jp (H. Haga)

16   Tel.: +81-11-706-4909

17

18

1   **<u>Abstract</u>**

2   Physical properties of the extracellular matrix (ECM) can control cellular phenotypes

3   via mechanotransduction, which is the process of translation of mechanical stresses into

4   biochemical signals. While current research is clarifying the relationship between

5   mechanotransduction and cytoskeleton or adhesion complexes, the contribution of transcription

6   factors to mechanotransduction is not well understood. The results of this study revealed that the

7   transcription factor NF-κB, a major regulator for immunoreaction and cancer progression, is

8   responsive to substrate stiffness. NF-κB activation was temporarily induced in H1299 lung

9   adenocarcinoma cells grown on a stiff substrate but not in cells grown on a soft substrate.

10   Although the activation of NF-κB was independent of the activity of integrin β1, an

11   ECM-binding protein, the activation was dependent on actomyosin contractions induced by

12   phosphorylation of myosin regulatory light chain (MRLC). Additionally, the inhibition of

13   MRLC phosphorylation by Rho kinase inhibitor Y27632 reduced the activity of NF-κB. We also

14   observed substrate-specific morphology of the cells, with cells grown on the soft substrate

15   appearing more rounded and cells grown on the stiff substrate appearing more spread out.

16   Inhibiting NF-κB activation caused a reversal of these morphologies on both substrates. These

17   results suggest that substrate stiffness regulates NF-κB activity via actomyosin contractions,

18   resulting in morphological changes.

19

1 **Keywords**

2 actomyosin; lung adenocarcinoma cell; NF-κB; mechanotransduction; substrate stiffness

3

4

1   **<u>Introduction</u>**

2   Mechanical cues, which include mechanical forces and physical properties of the

3   surrounding environment, modulate cellular phenotypes. For example, substrate stiffness affects

4   cell adhesion [1], direction of migration [2], and collectiveness of migration [3] in various cell

5   types. External deformation of an elastic substrate induces cellular stiffness responses in

6   fibroblasts [4]. In addition, mechanical cues regulate the differentiation state of mesenchymal

7   stem cells *in vitro* [5] and morphogenesis *in vivo* [6]. Mechanical cues are also related to

8   specific diseases [7]. In breast cancer, a stiffer extracellular matrix can induce more malignant

9   phenotypes [8]. In fibrosarcoma, mechanical stimuli increase the proportion of invading cells in

10   type I collagen/fibronectin matrices [9]. In blood vessels, extraordinary shear stress induces

11   atherosclerosis [10]. Thus, aberrant mechanical cues can affect cellular phenotypes and promote

12   certain types of diseases.

13   When cells sense mechanical cues, they convert them into biochemical signals. This

14   conversion is called "mechanotransduction." Previous studies have identified several molecules

15   whose primary responsibility is to sense mechanical stresses in cells. These molecules are called

16   "mechanosensors" and include molecules such as p130Cas [11] and filamin [12], which undergo

17   structural deformation in response to mechanical stresses in cells. Cells alter the protein

18   expression levels of adhesion complexes and reorganize their cytoskeletons, as a consequence

1   of sensing mechanical stresses [13]. Following this process, adhesion complexes and

2   cytoskeletons regulate cellular phenotypes such as migratory activity and morphology [1, 2].

3   Several primary and terminal mechanotransduction molecules have recently been identified [11,

4   12, 13], but the transcriptional molecules that regulate gene expression are not well understood.

5   The transcription factor NF-κB is a well-known regulator of immunoreaction and cancer

6   progression and responds to chemical stimuli, DNA damage, and reactive oxygen species.

7   Activated NF-κB induces the expression of cytokines (IL-1β, IL-8, etc.) and cancer regulatory

8   genes (TNFα, MMP9, etc.) [14, 15, 16, 17]. NF-κB consists of 5 subunits (RelA/p65, p105/p50,

9   p100/p52, RelB, and c-Rel), which form homo- or heterodimers [18]. Once the stimuli are

10   received, NF-κB dimers are translocated from the cytoplasm to the nucleus, where they function

11   as transcriptional activators. NF-κB activation is also induced by mechanical stresses such as

12   uniaxial stretch [19, 20] and shear stress [21].

13   Previous studies have suggested that NF-κB activation is regulated by various stimuli via

14   cytoskeleton and adhesion molecules. Actomyosin is one of these cytoskeletal complexes,

15   consisting of actin and myosin, which generates tensional force in cells. The tensional force in

16   actomyosin is regulated by phosphorylation of MRLC. Di-phosphorylated MRLC provokes

17   much stronger tensional force in actomyosin than mono- or non-phosphorylated MRLC does

18   [22]. Previous research has revealed that mechanical cues induce MRLC phosphorylation via

1 the RhoA signaling cascade [23]. Furthermore, MRLC regulates NF-κB activity by

2 TNFα-induced RhoA activation [24]. Integrins are heterodimeric glycoproteins that directly

3 bind extracellular matrices (ECM) and activate intracellular signaling pathways when they

4 connect to ECMs [25]. The heterodimers of integrins are composed of α and β chains. Integrin

5 β1 is a major component of the collagen receptor and has been reported to regulate NF-κB

6 activity [26, 27]. Thus, MRLC and integrin β1 are potential regulators of NF-κB activation by

7 mechanical stimuli.

8   Based on these previous studies, we proposed the hypothesis that substrate stiffness

9 regulates NF-κB activation and changes the expression of NF-κB-related genes. In this study,

10 we showed that stiff substrates induce temporary NF-κB activation and up-regulate IL-1β, IL-8,

11 and MMP9 mRNA expression in H1299 lung adenocarcinoma cells. Furthermore, NF-κB

12 activation does not require cell-substrate adhesion by integrin β1, but does require actomyosin

13 contraction depending on MRLC phosphorylation. Finally, NF-κB activity regulates cell

14 morphology, and high NF-κB activity induces cells to exhibit a spreading shape. These data

15 collectively suggest that NF-κB activation is triggered by a stiff substrate via cytoskeletal

16 tensions, leading to inflammatory reactions and spreading cell shape.

17

1   **Materials and Methods**

2   **Cell culture, reagents, antibodies, plasmids**

3   Human lung adenocarcinoma cell line H1299 cells were cultured in DMEM (Sigma, St.

4   Louis, MO) containing 10% FBS (BIST TECH) and 1% antibiotic/antimycotic solution (Sigma).

5   Monoclonal antibody AIIB2 (Developmental Studies Hybridoma Bank at the University of Iowa,

6   Iowa City, IA) was used for inhibition of integrin β1 activity. Y27632 (Sigma), blebbistatin

7   (TRC, Toronto, Canada), and 1-oleoyl-lysophosphatidic acid (LPA, Cayman Chemical, Ann

8   Arbor, MI) were used for Rho-associated protein kinase (ROCK) inhibition, myosin motor

9   activity inhibition, and Rho activation, respectively. Anti-NF-κB p65 (IBL, 18667), Alexa Fluor

10   594 goat anti-rabbit IgG (Invitrogen, Carlsbad, CA, A-11012), anti-paxillin monoclonal

11   antibody (BD Biosciences, San Jose, CA, 610052), phospho-myosin light chain 2 (Ser19/Thr18)

12   antibody (anti PP-MRLC; Cell Signaling Tech, Danvers, MA, #3674), Alexa Fluor 546 goat

13   anti-mouse IgG (Invitrogen, A-11003), and Alexa Fluor 546 goat anti-rabbit IgG (Invitrogen,

14   A-11010) were used for immunofluorescent staining and western blotting. Myosin light chain 2

15   antibody (anti-MRLC; Cell Signaling Tech, #3672), phospho-myosin light chain 2 (Ser19)

16   antibody (anti-P-MRLC; Cell Signaling Tech, #3671), anti-GAPDH (Ambion, Foster City, CA,

17   1103016), HRP anti-rabbit IgG (Cell Signaling Tech, #7074), and HRP anti-mouse IgG

18   (Bio-Rad Hercules, CA, 70-6516) were used for western blotting. MFP 488-phalloidin (Mo Bi

1   Tee, Göttingen, Germany) or Alexa Fluor 546 phalloidin (Invitrogen, A22283) was used for

2   F-actin staining. Rat NF-κB (p65) gene was obtained by RT-PCR from a cDNA library and

3   cloned into pDsRed-Monomer-N1 or pEGFP-N1 (BD Biosciences). For luciferase reporter

4   assay, pNF-κB-Luc, pTK-RL, and pcDNA3 plasmids were purchased from Stratagene, Promega,

5   and Invitrogen, respectively. Transfection of plasmids was performed with Lipofectamine 2000

6   (Invitrogen) or polyethyleneimine. For selection of transgenic cells, G418 (Promega, Madison,

7   WI) reagent was used at a concentration of 0.6–0.8 mg/mL. H-NLS or H1299-p65-1/p65-2 cells

8   were established by selecting the transgenic cells from H1299 cells transfected with NLS-venus

9   or Rat-p65wt-EGFP plasmid. Human TNFα (Cell Signaling Technology) and BAY-11-7082

10   (Sigma) were used for NF-κB activation and NF-κB inhibition, respectively.

11

12   **ECM coating and collagen gel substrates**

13   For stiff substrates, we prepared silanized cover glass (>1 GPa [8]) coated with type-I

14   collagen (Cell matrix I-C; Nitta Gelatin, Osaka, Japan). ECM-coated silanized cover glass is a

15   more stable and uniform ECM substrate than non-treated cover glass coated with the same ECM.

16   To prepare silanized cover glasses, we soaked cover glasses in saturated KOH in isopropanol

17   solution and incubated them overnight at room temperature. The cover glasses were washed 3

18   times   with   distilled   water   and   dried.   We   soaked   the   cover   glasses   in   0.33%

1 (3-aminopropyl)triethoxysilane in toluene solution and incubated them overnight at room

2 temperature. The cover glasses were washed 3 times with toluene and dried. For stiff substrates,

3 we also prepared collagen type-I-coated plastic dishes or 24-well plates (>1 GPa [8]). For soft

4 substrates, we prepared 1.6 mg/mL type-I collagen gels (approximately 0.6 kPa, based on

5 previously reported methods [28]; Cell matrix I-P, Nitta Gelatin). Plastic 24-well plates were

6 coated with fibronectin (Roche, Mannheim, Germany), laminin (Trevigen, Gaithersburg, MD),

7 or poly-L-lysine (Sigma), and used for ECM-coated stiff substrates.

8

9 **Polyacrylamide gel substrate**

10 Polyacrylamide gels were prepared as substrates of different stiffness [29]. The

11 stiffness of each gel was measured as previously reported [30]. Gels of 30.1 kPa (containing

12 0.16% N,N′-methylenebisacrylamide (BIS), 7.5% acrylamide, 115 mM

13 N-acryloyl-6-aminocaproic acid (ACA)), 2.0 kPa (containing 0.01% BIS, 7.5% acrylamide, 240

14 mM ACA), 13.8 kPa (containing 0.08% BIS, 7.5% acrylamide, 150 mM ACA), and 67.2 kPa

15 (containing 0.32% BIS, 7.5% acrylamide, 90 mM ACA) were polymerized for 1 h at room

16 temperature. The gels were fully hydrated in PBS and transferred to MES buffer (0.1 M MES,

17 0.5 M NaCl; pH, 6.1). Carboxyl groups of the ACA gels were activated with 0.2 M

18 1-ethyl-3-(3-dimethylaminopropyl)carbodiimide hydrochloride and 0.5 M

1   *N*-hydroxysuccinimide in MES buffer for 15 min at room temperature. The gels were then

2   washed with cold 70% methanol diluted with PBS before they were reacted with 0.2 mg/mL

3   type-I collagen (AteroCell IAC-50; KOKEN, Tokyo, Japan) in HEPES buffer (0.5 M HEPES;

4   pH 9.0) overnight at 4°C. Finally, the gels were transferred to 0.5 M ethanolamine in HEPES

5   buffer for reaction with any remaining active carboxyl groups. The gels were washed with

6   HEPES buffer and then 3 times with PBS. All gels were sterilized with UV light in a sterile

7   hood and equilibrated in culture medium before cell plating.

8

9   **Immunofluorescence staining**

10   H1299 and H1299-p65-2 cells ($1–2 \times 10^4$) were seeded on collagen-coated cover

11   glasses or collagen gels and cultured for 0.5, 2, 4, or 6 h. After culturing, the cells were fixed

12   with PFA (4%, room temperature, 10 min) and washed 3 times. Next, Triton-X100 (0.5%)

13   permeabilization was performed for 10 min at room temperature. The samples were washed 3

14   times. Blocking treatment with 0.5% BSA (for p65 and paxillin staining) or 0.5% skim milk

15   (PP-MRLC staining) in PBS was performed for 1 h at room temperature. Primary antibody

16   solution (p65 1:200 in PBS, paxillin 1:200 in PBS, PP-MRLC 1:150 with 0.5% skim milk in

17   PBS) was added for incubation overnight at 4°C. After 3 washes, secondary antibody solution

18   (Alexa Fluor 594 goat anti rabbit IgG 1:200 for p65 staining, Alexa Fluor 546 goat anti mouse

1   IgG, 1:500 for paxillin staining, Alexa Fluor 546 goat anti rabbit IgG, 1:500 for PP-MRLC

2   staining) with or without F-actin staining solution (MFP 488-phalloidin, 1:1000 or Alexa Fluor

3   546 phalloidin, 1:500) was added, and the mixtures were incubated for 1 h at room temperature.

4   After 3 washes, anti-fading solution (2.5% DABCO, 90% glycerol, 6% PBS; pH 8.0) was added.

5   The resulting images were captured with Nikon C1 or A1R confocal imaging system (Nikon

6   Instech., Tokyo, Japan) and edited with IMARIS software (Carl Zeiss, Oberkochen, Germany).

7   The proportion of NF-κB localization in the nucleus was calculated using Image J software as

8   the p65 intensity in the nucleus divided by the p65 intensity in the cytoplasm. The relative

9   number of the adhesion sites was calculated using Image-Pro software (Media Cybernetics Inc.,

10   Silver Spring, MD) as the number of paxillin dots in 1 cell divided by the cell area, evaluated

11   from F-actin or p65-EGFP fluorescent images. Statistical analysis was performed using

12   Student's t-test.

13

14   **Luciferase assay**

15   Luciferase plasmids (225 ng/mL pNF-κB-Luc, 2.25 ng/mL pTK-RL, and 900 ng/mL

16   pcDNA3) were transfected to semi-confluent H1299 cells on a plastic dish with Lipofectamine

17   2000. The medium was exchanged after 6 h, and after 24 h, it was changed to non-serum

18   DMEM, and the samples were incubated for 2 h. Cells were suspended and re-seeded and

1   luciferase activity was detected 6 h later by using Dual Luciferase Reporter Assay System

2   (Promega). Statistical analysis was performed using Student's t-test.

3

4   **Time-lapse fluorescent live imaging**

5   H1299-p65-1 cells were pre-incubated with non-serum DMEM for 2 h and

6   resuspended using serum-free medium. The cells were seeded with DMEM containing 10%

7   FBS on collagen-coated cover glasses or collagen gels. The samples were filled with the

8   DMEM and sealed with silicone grease to avoid changes in the pH of the medium. p65-EGFP

9   fluorescent images were observed with Nikon A1R confocal imaging system (Nikon Instech.).

10 Images were captured every 10 min, and three-dimensional images and movies were edited with

11 IMARIS software. The fluorescent intensity of p65-EGFP in the nucleus was calculated using

12 Image J software. The relative intensities of PP-MRLC were evaluated from the fluorescent

13 intensity ratio of PP-MRLC/GAPDH calculated by Image-Pro software (Media Cybernetics

14 Inc.). Statistical analysis was performed using Student's t-test.

15

16 **Western blotting**

17 Cell lysates were prepared in SDS sample buffer (0.25 M Tris-HCl, 5% dithiothreitol,

18 2.3% sodium dodecyl sulfate, 10% glycerol, 0.01% bromophenol blue, pH 8.8) and separated on

1   polyacrylamide gels. For the detection of MRLC, P-MRLC, and PP-MRLC, the cells were fixed

2   with 10% trichloroacetic acid in PBS and washed 3 times before lysis. When we prepared the

3   lysates from the cells on a collagen gel, we treated the cells with 0.5% collagenase (Nitta

4   Gelatin) in PBS for 1 h at 37°C to remove the collagen gel before lysis. Lysates were treated

5   with supersonic wave treatment and boiled for 5 min. Polyacrylamide gels (10% for p65 and

6   GAPDH, 12.5% for MRLC, P-MRLC, PP-MRLC, and GAPDH) were prepared for SDS-PAGE

7   (20 mA per gel, 1 h). Following SDS-PAGE, blotting to PVDF membranes was performed (92

8   mA per gel, 30 min for p65 and GAPDH, 1 h for MRLC, P-MRLC, PP-MRLC, and GAPDH).

9   After blotting, the membranes were incubated in 5% skim milk in TBS-Tween solution for 1 h

10   at room temperature. Membranes were incubated with primary antibodies (p65 1:1000, MRLC

11   1:1000, P-MRLC 1:300, PP-MRLC 1:300–1:600, and GAPDH 1:1000000–1:10000000)

12   overnight at 4°C. After 3 washes, membranes were incubated with secondary antibodies (HRP

13   anti-rabbit IgG 1:10000 for p65, MRLC, P-MRLC, and PP-MRLC; HRP anti-mouse IgG

14   1:200000 for GAPDH) for 1 h at room temperature. Signals were detected with Immobilon

15   Western Chemiluminescent HRP substrate (Millipore). The relative expressions of the proteins

16   were evaluated from intensity of the proteins/GAPDH ratios calculated by Image J software.

17   Statistical analysis was performed using Student's t-test.

18

1 **RT-PCR**

2 H1299 cells (3×10^5) were seeded onto each substrate and incubated at 37°C. RNAs

3 were isolated 6 h later using TriPure isolation Reagent (Roche). The isolating manipulation was

4 performed twice to ensure removal of any contaminating DNA or protein. cDNA were generated

5 with RevTra Ace kit (TOYOBO, Osaka, Japan), and PCR was performed with Taq polymerase

6 with ThermoPol Buffer (NEB, Ipswich, MA). The following primers were used:

7 GAPDH, 5′-ACCACAGTCCATGCCATCAC-3′ (upper) and

8 5′-TCCACCACCCTGTTGCTGTA-3′ (lower); IL-1β, 5′-TGCACGCTCCGGGACTCACA-3′

9 (upper) and 5′-AGGCAGGCAGTTGGGCATTGG-3′ (lower); IL-8,

10 5′-GTGGACCACACTGCGCCAACA-3′ (upper) and 5′-GGCCCTTGGCCTCAATTTTGCT-3′

11 (lower); and MMP9, 5′-GACACCTCTGCCCTCACCATGAG-3′ (upper) and

12 5′-AGAAGCCAAACCGGTCGTCGG-3′ (lower). The relative expressions of inflammatory

13 genes were evaluated from intensity of the genes/GAPDH ratios calculated by Image J software.

14 Statistical analysis was performed using Student's t-test.

15

16 **Adhesion area assay**

17 For assay of H1299, H-NLS, and H1299-p65-2 cells, 1×10^5 cells were seeded onto

18 plastic dishes coated with collagen or collagen gels, or 1×10^4 cells were seeded onto

1 collagen-coated cover glass. For assay of the cells expressing DsRed or p65DN plasmids, the

2 plasmids were transfected into semi-confluent H1299 cells with polyethyleneimine. After 1-day

3 incubation, cells were resuspended and re-seeded (1×10^4 cells) on collagen gels or plastic

4 24-well plates coated with collagen. Following incubation, phase-contrast images and

5 fluorescent images were captured by a TE300 phase-contrast microscope with a 10× objective

6 (Nikon Instech.) or an EVOS microscope with a 20× objective (AMG, Bothell, WA). Cell

7 adhesion areas were calculated by ImageJ software. Statistical analysis was performed using

8 Student's t-test.

9

10 **Adhesion ability assay**

11   H-NLS and H1299-p65-2 cells (1.5×10^5) were seeded onto a plastic 96-well plate

12 coated with collagen or onto a 0.6-kPa collagen gel. Plates were then centrifuged at 2000 rpm

13 for 35 s at room temperature and incubated at 37°C. After 30 min, the wells were washed 3

14 times with PBS. The images of adhering cells on the well were captured by a TE300

15 phase-contrast microscope with a 10× objective (Nikon Instech.). The relative number of

16 adhering cells was evaluated by calculating the number of cells per field of the images.

17

1 **Results**

2 **Substrate stiffness regulates temporary activation of NF-κB**

3   Because NF-κB is translocated from the cytoplasm to the nucleus and functions as a

4 transcription factor when cells receive certain stimuli [18], we observed NF-κB localization in

5 NLS-venus transgenic H1299 (H-NLS) cells on stiff or soft substrates. For the stiff substrate, we

6 used a cover glass coated with type-I collagen (>1 GPa). For the soft substrate, we prepared 1.6

7 mg/mL type-I collagen gel (0.6 kPa). Cells exhibited a higher rate of NF-κB localization to the

8 nucleus 2–6 h after seeding on the stiff substrate than on the soft substrate (Fig. 1A, B). The

9 transcriptional activity of NF-κB detected by luciferase reporter assay was also higher in the

10 cells grown on the stiff substrate than on the soft substrate (Fig. 1C). For the luciferase reporter

11 assay, we used 30.1-kPa polyacrylamide gels containing 0.16% *N*,*N*′-methylenebisacrylamide

12 (BIS) as the stiff substrate and 2.0-kPa polyacrylamide gels containing 0.01% BIS as the soft

13 substrate. The differences in NF-κB localization detected by immunofluorescence staining

14 between cells on stiff and soft substrates were smaller than those in NF-κB activity detected by

15 luciferase reporter assay, but this may be due to differences in experimental design. The

16 differences in NF-κB activity detected by luciferase reporter assay reflected the transcriptional

17 activity at 6 h after seeding, while conversely, NF-κB localization was observed at a single time

18 point by immunofluorescence staining. Thus, we suggest that the differences in NF-κB activity

1   detected by luciferase assay indicated total differences for 6 h and indicated larger differences

2   than NF-κB localization did at a single time point.

3   To investigate the dose responsivity of NF-κB activity to substrate stiffness, we

4   performed luciferase reporter assay using polyacrylamide gels of 2.0, 13.8, 30.1, 67.2 kPa

5   stiffness. The NF-κB activities of H1299 cells on 30.1- and 67.2-kPa gels were higher than

6   those on 2.0- and 13.8-kPa gels (Fig. S1). This result indicates that substrate stiffness between

7   13.8 and 30.1 kPa is critical to activate NF-κB for H1299 cells.

8   In addition, to observing the time-course of NF-κB localization in living cells, we

9   performed time-lapsed fluorescent live imaging. To observe the localization of NF-κB in living

10   cells, we established 2 cell lines, H1299-p65-1 and H1299-p65-2, which resulted from the

11   sub-cloning of transgenic H1299 cells expressing NF-κB (p65)-EGFP. We used H1299-p65-1

12   cells for the fluorescent live imaging, because these cells showed more normal NF-κB activity

13   than H1299-p65-2 cells (Fig. S2A). On the stiff (>1 GPa) substrate, p65-EGFP fluorescent

14   intensity in the nucleus was increased from 0 to 1.5 h after seeding. From 4.5 to 6 h after

15   seeding, the intensity began to decrease (Fig. 2A, B, Video S1). On the soft (0.6 kPa) substrate,

16   p65-EGFP intensity in the nucleus exhibited almost no change after seeding (Fig. 2A, B, Video

17   S2).

18   To investigate whether the changes in NF-κB nuclear localization depended on the

1   amount of NF-κB protein in the cells, we examined protein expression by western blotting and

2   found no significant differences between cells grown on stiff (30.1 kPa) versus soft (2.0 kPa)

3   substrates (Fig. S3). These data suggest that NF-κB is temporarily activated in H1299 cells

4   grown on the stiff substrate.

5

6   **Substrate stiffness and NF-κB activity regulate the expression of inflammatory genes**

7   Next, we investigated gene expression regulated by substrate stiffness and NF-κB

8   activity. Because IL-1β [31], IL-8 [32], and MMP9 [33] are known to be upregulated by NF-κB

9   activation, RT-PCR was performed to detect the mRNA expression of these genes. IL-1β, IL-8,

10   and MMP9 expressions were upregulated to a greater extent in H1299 cells grown on a stiff (>1

11   GPa) substrate compared with cells grown on a soft (0.6 kPa) substrate 6 h after seeding,

12   although the differences for IL-8 were not significant (Fig. 3A, B). Furthermore, H1299-p65-2

13   cells, which showed higher NF-κB activity than H-NLS cells (Fig. S2B), expressed higher

14   levels of IL-1β, IL-8, and MMP9 mRNA than did H-NLS cells grown on a soft (0.6 kPa)

15   substrate, although the differences for IL-1β were not significant (Fig. 3C, D). These results

16   indicate that substrate stiffness regulates the NF-κB-dependent mRNA expressions of IL-1β,

17   IL-8, and MMP9 in H1299 cells.

18

1   **NF-κB activation by stiff substrates is independent of adhesion molecules**

2   Next, we examined which molecules are regulated by substrate stiffness, thus inducing

3   NF-κB activation. To adhere to the substrates, cells form a linkage between ECM proteins and

4   adhesion molecules [25]. Integrin β1 plays a major role in the connection between cells and

5   type-I collagen, which is an abundant component of connective tissues. Integrin β1 is also

6   reported to induce NF-κB activation in response to mechanical stimuli [26, 27]. Because of this

7   property of integrin β1, we evaluated NF-κB activity in H1299 cells cultured with or without

8   monoclonal antibody AIIB2, which inhibits integrin β1 activity [34]. AIIB2 treatment did not

9   reduce the proportion of cells adhered to the substrate, but did cause significant changes in cell

10   morphology compared with non-treated cells (Fig. S4A, B). However, there was no significant

11   difference in NF-κB activity between the cells treated with AIIB2 and the non-treated cells (Fig.

12   S4C). In addition, H1299 cells cultured on a plastic substrate coated with poly-L-lysine,

13   fibronectin, laminin, or collagen showed no remarkable differences in NF-κB activity (Fig.

14   S4D). These results suggest that NF-κB activation in H1299 cells grown on a stiff substrate may

15   not be regulated by adhesion molecules such as integrin β1 and ECM molecules.

16

17

18

Actomyosins are regulated by substrate stiffness and induce NF-κB activation

Next, we focused on actomyosin, a cytoskeletal complex generating cellular contractile forces. Treatment with Y27632—a ROCK inhibitor—or blebbistatin (a myosin II inhibitor) inhibited actomyosin contractions and significantly decreased NF-κB activity in cells grown on a stiff (>1 GPa) substrate (Fig. 4A). Furthermore, treatment with lysophosphatidic acid (LPA) (an inducer of RhoA activation) increased NF-κB activity on a soft (0.6 kPa) substrate (Fig. 4A). These results indicate that actomyosin contractions lead to NF-κB activation.

For observation of actomyosin contractile forces, we performed di-phosphorylated MRLC (PP-MRLC) immunofluorescent staining in the cells 45 min after seeding on stiff (>1 GPa) or soft (0.6 kPa) substrates. PP-MRLC localization indicates local contractile sites, generated by actomyosins [22]. On a soft (0.6 kPa) substrate, localization of PP-MRLC was not observed (Fig. 4B). In contrast, on a stiff (>1 GPa) substrate, PP-MRLC was localized at the bottom of the cell periphery (Fig. 4B). The relative fluorescent intensity of PP-MRLC per F-actin was higher in the cells on a stiff (>1 GPa) substrate than in the cells on a soft (0.6 kPa) substrate (Fig. 4C). Western blotting analysis also indicated that MRLC was significantly more di- or mono-phosphorylated on a stiff (30.1 kPa) substrate than on a soft (2.0 kPa) substrate 45 min after seeding (Fig. 4D, E). In addition, western blotting analysis indiccated that Y27632

1   treatment reduced PP-MRLC on both stiff (>1 GPa) and soft (0.6 kPa) substrates whereas LPA

2   treatment increased PP-MRLC on only a soft (0.6 kPa) substrate (Fig. S5). Taken together, these

3   data suggest that stiff substrates induce actomyosin contractions generated by MRLC

4   phosphorylation, leading to NF-κB activation in H1299 cells.

5   In contrast, NF-κB activation did not induce reconstruction of F-actin and MRLC

6   di-phosphorylation. F-actin localization detected by fluorescence staining was similar in H1299

7   and H1299-p65-2 cells, which showed higher NF-κB activity than H1299 cells (Fig. S2A) on

8   both stiff (>1 GPa) and soft (0.6 kPa) substrates (Fig. S6A). Conversely, H1299-p65-2 cells

9   exhibited higher PP-MRLC signal on a stiff (>1 GPa) substrate than on a soft (0.6 kPa) substrate,

10   as well as in H1299 cells (Fig. S6A). Western blotting analysis indicated that H1299-p65-2 cells

11   showed lower PP-MRLC expression than H-NLS cells on a soft (2.0 kPa) substrate (Fig. S6B).

12   These results suggest that NF-κB activation does not induce MRLC di-phosphorylation in

13   H1299 cells.

14

15   **NF-κB activation induces cell spreading in H1299 cells**

16   Next, we investigated the cellular phenotype affected by NF-κB activation in H1299

17   cells grown on stiff or soft substrates. On a stiff (>1 GPa and 30.1 kPa) substrate, H1299 cells

18   exhibited a higher degree of spreading than they did on a soft (2.0 and 0.6 kPa) substrate (Fig.

1   5A, B and Fig. S7, 8). To examine the contribution of NF-κB activity on cell morphology, we

2   transfected dominant-negative mutant p65 conjugated with DsRed (p65DN) or DsRed backbone

3   plasmids into H1299 cells and analyzed the morphology of the cells. Cells transfected with

4   p65DN exhibited lower NF-κB activity (Fig. S9) and less spreading compared to DsRed

5   transfected cells when grown on a stiff (>1 GPa) substrate (Fig. 5C, D and Fig. S7). In contrast,

6   H1299-p65-1 and H1299-p65-2 cells, which showed higher activity of NF-κB than H-NLS cells

7   on a soft (0.6 kPa) substrate (Fig. S2B), showed more cell spreading than H-NLS cells on a soft

8   (0.6 kPa) substrate (Fig. 5E, F and Fig. S7). We also treated cells with TNFα, and found that

9   TNFα induced NF-κB activation and spreading shape in cells grown on a soft (0.6 kPa)

10   substrate (Fig. S10A, B, C; S11A, B). In addition, we treated cells with BAY-11-7082, which

11   inhibited NF-κB activity induced by TNFα (Fig. S10D, E). The effect of TNFα on cellular

12   morphology was inhibited by BAY-11-7082 treatment (Fig. S11C). In contrast to NF-κB

13   activation and cell spreading, TNFα did not affect F-actin localization or MRLC

14   di-phosphorylation on soft substrates (Fig. S12). Thus, TNFα may induce NF-κB activation and

15   cell spreading, independent of actomyosin contractions. Collectively these data suggest that

16   NF-κB activation induces morphological changes.

17

18

1 **Adhesion ability in H1299 cells is promoted by NF-κB activity**

2   Next, we evaluated adhesion ability in H-NLS and H1299-p65-2 cells, which

3 exhibited higher NF-κB activity than H-NLS cells (Fig. S2B) with both stiff and soft substrates.

4 H1299-p65-2 showed greater adhesion ability than H-NLS cells on stiff (>1 GPa) and soft (0.6

5 kPa) substrates (Fig. S13). This result indicates that NF-κB activity promotes both spreading

6 and adhesion ability in H1299 cells. Conversely, in contrast to cell spreading, adhesion abilities

7 of H-NLS and H1299-p65-2 were higher on a soft (0.6 kPa) substrate compared than on a stiff

8 (>1 GPa) substrate (Fig. S13). Taken together, these results indicate that stiff substrates increase

9 cell spreading and decrease cell adhesion ability in H1299 cells, and that cell spreading is

10 regulated by a mechanism other than molecular signaling, as evidenced by the strength of

11 cell-substrate adhesion.

12

13 **Actomyosin contractions regulate the formation of focal adhesions independent on NF-κB**

14 **activity**

15   Because the formation of focal adhesions is upregulated by stiff substrate and

16 actomyosin contractions [13, 35], we investigated whether focal adhesions were also regulated

17 by substrate stiffness and actomyosin contractions in our experimental system. Focal adhesions

18 were observed by immunofluorescence staining of paxillin, which is a component protein of

1   focal adhesion [36]. H1299 cells exhibited more focal adhesions (paxillin dots) on a stiff (>1

2   GPa) substrate than on a soft (0.6 kPa) substrate (Fig. S14A, B). Furthermore, Y27632 and

3   blebbistatin treatment reduced the number of focal adhesions in H1299 cells on stiff (>1 GPa)

4   and/or soft (0.6 kPa) substrates (Fig. S14A, B). Several H1299 cells treated with LPA on a soft

5   (0.6 kPa) substrate increased focal adhesions, although the difference was not significant (Fig.

6   S14A, B).

7   Next, we investigated whether the formation of focal adhesions was regulated by

8   NF-κB activity. H1299-p65-2 cells, which exhibited higher NF-κB activity than H1299 cells

9   (Fig. S2A) on a soft (0.6 kPa) substrate, produced fewer focal adhesions than on a stiff (>1 GPa)

10   substrate, and this was also observed with H1299 cells (Fig. S15A, B). These results suggest

11   that substrate stiffness regulates the formation of focal adhesions via actomyosin contraction in

12   H1299 cells, independent on NF-κB activity.

13

14   **Actomyosin contractions regulate cell spreading in H1299 cells**

15   To evaluate the effects of actomyosin on cell spreading in H1299 cells, we calculated

16   cell area in H1299 cells treated with Y27632, blebbistatin, and LPA. F-actin distributions, which

17   are important for maintenance of cell shape, were similar in H1299 cells (both treated and

18   non-treated with these drugs) on stiff (>1 GPa) and soft (0.6 kPa) substrates (Fig. S14A).

1   Blebbistatin treatment slightly decreased cell area in H1299 cells on a stiff (>1 GPa) substrate,

2   although the difference was not comparatively significant (Fig. S14C). This result suggests that

3   actomyosin plays an important role for maintaining cell spreading in H1299 cells on a stiff

4   substrate. In addition, blebbistatin and LPA treatment increased the cell area in H1299 cells on a

5   soft (0.6 kPa) substrate (Fig. S14C), and these results further suggest that actomyosin

6   contractions regulate cell spreading in H1299 cells.

7

8

1   **<u>Discussion</u>**

2   The results of this study showed that substrate stiffness regulates NF-κB activation in

3   H1299 cells. When grown on a stiff (>1 GPa, 67.2 kPa, and 30.1 kPa) substrate, the cells

4   activated NF-κB, while on a soft (13.8, 2.0, and 0.6 kPa) substrate, the cells exhibited only low

5   levels of NF-κB activity. While biochemical stimuli [18] and mechanical forces [19, 20, 21]

6   have been shown to induce NF-κB activation, the effects of substrate stiffness on NF-κB

7   activation have not been studied well. To our knowledge, this is the first study to reveal that

8   substrate stiffness regulates NF-κB activation.

9   The results of a previous study have indicated that stiffness of normal lung tissue is

10   approximately 2.0 kPa [37], while another study showed that tissue stiffening promotes

11   malignancy in breast cancer [38]. We demonstrated in this study that H1299 lung cancer cells

12   exhibit lower NF-κB activity on the soft substrates (~2.0 kPa) than on the stiff substrates (30.1

13   kPa). Since it is known that NF-κB plays an important role in cancer progression [15], our

14   results suggest that an abnormally stiff environment in lung tissue promotes malignancy in lung

15   cancer cells via NF-κB activation.

16   Additionally, we demonstrated that the NF-κB activation regulated by substrate stiffness

17   is a temporary event, which is consistent with the findings from a previous study indicating that

18   NF-κB activation in response to various stimuli is typically temporary [39]. Similarly, we

1   observed temporary NF-κB activation by stiff substrates 2–6 h after seeding. A previous study

2   showed that YAP/TAZ, which is the first reported transcription factor regulated by substrate

3   stiffness, was activated 48 h after the cells were seeded on a stiff substrate [40]. In this study,

4   NF-κB activation did not significantly differ between the cells grown on stiff versus soft

5   substrates at 48 h after seeding. Thus, while both YAP/TAZ and NF-κB act as

6   mechanotransductive transcription factors, the time courses of their activation are entirely

7   different.

8   In this study, we further demonstrated that NF-κB activation is induced by substrate

9   stiffness. However, this activation was weaker than the NF-κB activation by TNF-α treatment.

10   This may be because NF-κB activation by mechanical stress is weaker than that by biochemical

11   stimuli. A previous study showed that the activation of NF-κB by cyclic stretch, a mechanical

12   stress, is weaker than the activation by IL-1, a biochemical stimulus [20]. Thus, the activation of

13   NF-κB by substrate stiffness, a mechanical stress, may be weaker than that by TNF-α, a

14   biochemical stimulus.

15   Stiff substrates activate NF-κB, and as a result, induce the expression of inflammatory

16   genes such as IL-1β, IL-8, and MMP9. These genes are known to facilitate migration, invasion,

17   and metastasis in cancer cells [33, 39, 41], suggesting that substrate stiffness may regulate

18   cancer malignancy via the expression of these genes.

1   To better understand the possible relationship between NF-κB activation and the

2 migratory and invasive potential of cells, we examined several mechanisms controlling cell

3 adhesion and movement. Interestingly, we found that NF-κB activation in H1299 cells was not

4 dependent on adhesion molecules such as integrin β1 and ECM molecules. The inhibition of

5 integrin β1 activity by AIIB2 treatment induced round morphology of H1299 cells grown on a

6 stiff substrate. Thus, activation of integrin β1 may induce a spreading morphology of H1299

7 cells via cell-substrate adhesion. On the other hand, integrin β1 inhibition by AIIB2 did not

8 suppress NF-κB activation. Furthermore, H1299 cells grown on poly-L-lysine, fibronectin,

9 laminin, or collagen substrates exhibited no remarkable differences in NF-κB activity. These

10 results indicate that the extension of the cells and the interactions of integrin β1 with ECM may

11 not play important roles in NF-κB activation. Thus, H1299 cells may sense substrate stiffness

12 through a mechanism independent of cell-substrate adhesion to regulate NF-κB activity.

13   Stiff substrates induce actomyosin contractile forces, which, in turn, trigger NF-κB

14 activation. Previous research has shown that stiff substrates increase the traction forces

15 generated by actomyosins [42], further enhancing NF-κB activation. Here, we showed that stiff

16 substrates induced MRLC di-phosphorylation at the bottom of the cell periphery 45 min after

17 seeding H1299 cells. Furthermore, we showed that actomyosin contractile forces triggered

18 NF-κB activation by using Y27632 as a ROCK inhibitor, blebbistatin as a myosin II inhibitor, or

1   LPA as a Rho activator. However, the differences in NF-κB activity among H1299 cells treated

2   with Y27632, blebbistatin, and LPA were small. This may be because the drug treatments are

3   not sufficient to regulate the entire activation of NF-κB by a stiff substrate. It is therefore

4   possible that there may be an actomyosin-independent signaling cascade to regulate NF-κB

5   activity by substrate stiffness. On the other hand, previous study reported that NF-κB activation

6   induced by TNFα stimuli requires MRLC phosphorylation in renal endothelial cells [24].

7   However, in this study, TNFα stimuli did not induce MRLC di-phosphorylation in H1299 cells.

8   MRLC may regulate NF-κB activation induced by mechanical stimuli whereas MRLC may not

9   induce NF-κB activation by chemical stimuli in H1299 cells.

10   Stiff substrates appear to induce cell spreading via NF-κB activation. A previous study

11   revealed that substrate stiffness regulates cell adhesion area by modulating adhesion and

12   cytoskeletal molecules in MCF10A breast epithelial cells [42]. Therefore, spreading of H1299

13   cells regulated by NF-κB may depend on the molecules that induce cell extension, such as

14   molecules related to cytoskeletons or adhesion complexes. However, in this study, we

15   demonstrated that NF-κB activation did not increase the formation of focal adhesions, whereas

16   Y27632, blebbistatin, and LPA treatment did affect the formation of NF-κB in H1299 cells.

17   Thus, substrate stiffness regulates the formation of focal adhesions via actomyosin contractions,

18   independent of NF-κB activation. Furthermore, NF-κB activation did not induce MRLC

1   di-phosphorylation and reconstruction of actin filament in H1299 cells. Cell spreading in H1299

2   cells induced by NF-κB activation may therefore be triggered by another adhesion molecule

3   and/or cytoskeleton.

4   *In vivo*, many types of cells, including cancer cells, adhere to their substrates, which

5   include collagen-rich connective tissues such as basement membrane. A previous study showed

6   that stiffened substrates induce cancer progression *in vivo* and the substrates are stiffened by

7   expression of lysyl oxidase (LOX), which involves crosslinking of collagen fibers [38]. Thus,

8   LOX may be a good target for cancer therapies, although there have been no reports on the use

9   of LOX-targeting therapies in clinical practice. Our study indicated that stiff substrates trigger

10   activation of NF-κB in H1299 lung adenocarcinoma cells. In addition, previous studies have

11   shown that inhibition of NF-κB is effective in cancer therapies [43]. Thus, combined therapies

12   targeting LOX with NF-κB inhibitors may be more effective than stand-alone therapy.

13   In summary, we showed that substrate stiffness regulated temporary NF-κB activation via

14   actomyosin contractions in H1299 cells. The activation of NF-κB appeared to trigger the

15   expression of inflammatory genes. Furthermore, NF-κB activation induced a spreading

16   morphology, which may be caused by inflammatory genes. These results suggest that when lung

17   cancer cells are exposed to stiff substrates, the cells may induce NF-κB activation and, as a

18   result, modulate inflammatory reactions and cancer progression. Therefore, substrate stiffness

1   and NF-κB may be good targets to explore for cancer therapy.

2

9

10

1   **References**

2   [1]   T. Yeung, P.C. Georges, L.A. Flanagan, B. Marg, M. Ortiz, M. Funaki, N. Zahir, W.

3   Ming, V. Weaver, P.A. Janmey, Effects of substrate stiffness on cell morphology,

4   cytoskeletal structure, and adhesion, Cell Motil Cytoskeleton 60 (2005) 24-34.

5   [2]   C.M. Lo, H.B. Wang, M. Dembo, Y.L. Wang, Cell movement is guided by the rigidity

6   of the substrate, Biophys J 79 (2000) 144-152.

7   [3]   H. Haga, C. Irahara, R. Kobayashi, T. Nakagaki, K. Kawabata, Collective movement of

8   epithelial cells on a collagen gel substrate, Biophys J 88 (2005) 2250-2256.

9   [4]   T. Mizutani, H. Haga, K. Kawabata, Cellular stiffness response to external deformation:

10   tensional homeostasis in a single fibroblast, Cell Motil Cytoskeleton 59 (2004) 242-248.

11   [5]   A.J. Engler, S. Sen, H.L. Sweeney, D.E. Discher, Matrix elasticity directs stem cell

12   lineage specification, Cell 126 (2006) 677-689.

13   [6]   H. Zhang, F. Landmann, H. Zahreddine, D. Rodriguez, M. Koch, M. Labouesse, A

14   tension-induced mechanotransduction pathway promotes epithelial morphogenesis,

15   Nature 471 (2011) 99-103.

16   [7]   P.A. Janmey, R.T. Miller, Mechanisms of mechanical signaling in development and

17   disease, J Cell Sci 124 (2011) 9-18.

18   [8]   D.T. Butcher, T. Alliston, V.M. Weaver, A tense situation: forcing tumour progression,

1   Nat Rev Cancer 9 (2009) 108-122.

2 [9] S. Menon, K.A. Beningo, Cancer cell invasion is enhanced by applied mechanical

3   stimulation, PLoS One 6 (2011) e17277.

4 [10] E. Hergenreider, S. Heydt, K. Tréguer, T. Boettger, A.J. Horrevoets, A.M. Zeiher, M.P.

5   Scheffer, A.S. Frangakis, X. Yin, M. Mayr, T. Braun, C. Urbich, R.A. Boon, S.

6   Dimmeler, Atheroprotective communication between endothelial cells and smooth

7   muscle cells through miRNAs, Nat Cell Biol 14 (2012) 249-256.

8 [11] Y. Sawada, M. Tamada, B.J. Dubin-Thaler, O. Cherniavskaya, R. Sakai, S. Tanaka, M.P.

9   Sheetz, Force sensing by mechanical extension of the Src family kinase substrate

10   p130Cas, Cell 127 (2006) 1015-1026.

11 [12] A.J. Ehrlicher, F. Nakamura, J.H. Hartwig, D.A. Weitz, T.P. Stossel, Mechanical strain

12   in actin networks regulates FilGAP and integrin binding to filamin A, Nature 478 (2011)

13   260-263.

14 [13] Y.K. Wang, Y.H. Wang, C.Z. Wang, J.M. Sung, W.T. Chiu, S.H. Lin, Y.H. Chang, M.J.

15   Tang, Rigidity of collagen fibrils controls collagen gel-induced down-regulation of

16   focal adhesion complex proteins mediated by alpha2beta1 integrin, J Biol Chem 278

17   (2003) 21886-21892.

18 [14] Q. Li, I.M. Verma, NF-kappaB regulation in the immune system, Nat Rev Immunol 2

1   (2002) 725-734.

2 [15] M. Karin, Y. Cao, F.R. Greten, Z.W. Li, NF-kappaB in cancer: from innocent bystander

3   to major culprit, Nat Rev Cancer 2 (2002) 301-310.

4 [16] D. Sliva, M.T. Rizzo, D. English, Phosphatidylinositol 3-kinase and NF-kappaB

5   regulate motility of invasive MDA-MB-231 human breast cancer cells by the secretion

6   of urokinase-type plasminogen activator, J Biol Chem 277 (2002) 3150-3157.

7 [17] Y. Saitoh, V.J. Martínez Bruyn, S. Uota, A. Hasegawa, N. Yamamoto, I. Imoto, J.

8   Inazawa, S. Yamaoka, Overexpression of NF-κB inducing kinase underlies constitutive

9   NF-κB activation in lung cancer cells, Lung Cancer 70 (2010) 263-270.

10 [18] M.S. Hayden, S. Ghosh, Signaling to NF-kappaB, Genes Dev 18 (2004) 2195-2224.

11 [19] W. Du, I. Mills, B.E. Sumpio, Cyclic strain causes heterogeneous induction of

12   transcription factors, AP-1, CRE binding protein and NF-kB, in endothelial cells:

13   species and vascular bed diversity, J Biomech 28 (1995) 1485-1491.

14 [20] H. Inoh, N. Ishiguro, S. Sawazaki, H. Amma, M. Miyazu, H. Iwata, M. Sokabe, K.

15   Naruse, Uni-axial cyclic stretch induces the activation of transcription factor nuclear

16   factor kappaB in human fibroblast cells, FASEB J 16 (2002) 405-407.

17 [21] C. Hahn, M.A. Schwartz, The role of cellular adaptation to mechanical forces in

18   atherosclerosis, Arterioscler Thromb Vasc Biol 28 (2008) 2101-2107.

1   [22]   T. Mizutani, H. Haga, Y. Koyama, M. Takahashi, K. Kawabata, Diphosphorylation of

2   the myosin regulatory light chain enhances the tension acting on stress fibers in

3   fibroblasts, J Cell Physiol 209 (2006) 726-731.

4   [23]   T. Mizutani, K. Kawabata, Y. Koyama, M. Takahashi, H. Haga, Regulation of cellular

5   contractile force in response to mechanical stretch by diphosphorylation of myosin

6   regulatory light chain via RhoA signaling cascade, Cell Motil Cytoskeleton 66 (2009)

7   389-397.

8   [24]   X. Wu, R. Guo, P. Chen, Q. Wang, P.N. Cunningham, TNF induces caspase-dependent

9   inflammation in renal endothelial cells through a Rho- and myosin light chain

10   kinase-dependent mechanism, Am J Physiol Renal Physiol 297 (2009) F316-326.

11 [25]   R.O. Hynes, Integrins: bidirectional, allosteric signaling machines, Cell 110 (2002)

12   673-687.

13 [26]   E. Tzima, M.A. Del Pozo, W.B. Kiosses, S.A. Mohamed, S. Li, S. Chien, M.A.

14   Schwartz, Activation of Rac1 by shear stress in endothelial cells mediates both

15   cytoskeletal reorganization and effects on gene expression, EMBO J 21 (2002)

16   6791-6800.

17 [27]   T. Petzold, A.W. Orr, C. Hahn, K.A. Jhaveri, J.T. Parsons, M.A. Schwartz, Focal

18   adhesion kinase modulates activation of NF-kappaB by flow in endothelial cells, Am J

1   Physiol Cell Physiol 297 (2009) C814-822.

2 [28] T. Mizutani, H. Haga, K. Kato, K. Matsuda, K. Kawabata, Observation of stiff domain

3   structure on collagen gels by wide-range scanning probe microscopy, Japanese Journal

4   of Applied Physics Part 1-Regular Papers Brief Communications & Review Papers 45

5   (2006) 2353-2356.

6 [29] R.J. Pelham, Y. Wang, Cell locomotion and focal adhesions are regulated by substrate

7   flexibility, Proc Natl Acad Sci U S A 94 (1997) 13661-13665.

8 [30] T. Shimizu, J. Ueda, J.C. Ho, K. Iwasaki, L. Poellinger, I. Harada, Y. Sawada, Dual

9   inhibition of Src and GSK3 maintains mouse embryonic stem cells, whose

10   differentiation is mechanically regulated by Src signaling, Stem Cells 30 (2012)

11   1394-1404.

12 [31] J.P. Cogswell, M.M. Godlevski, G.B. Wisely, W.C. Clay, L.M. Leesnitzer, J.P. Ways, J.G.

13   Gray, NF-kappa B regulates IL-1 beta transcription through a consensus NF-kappa B

14   binding site and a nonconsensus CRE-like site, J Immunol 153 (1994) 712-723.

15 [32] M.A. Fiedler, K. Wernke-Dollries, J.M. Stark, Inhibition of TNF-alpha-induced

16   NF-kappaB activation and IL-8 release in A549 cells with the proteasome inhibitor

17   MG-132, Am J Respir Cell Mol Biol 19 (1998) 259-268.

18 [33] C.H. Tang, T.W. Tan, W.M. Fu, R.S. Yang, Involvement of matrix metalloproteinase-9

1   in stromal cell-derived factor-1/CXCR4 pathway of lung cancer metastasis,

2   Carcinogenesis 29 (2008) 35-43.

3 [34] Z. Werb, P.M. Tremble, O. Behrendtsen, E. Crowley, C.H. Damsky, Signal transduction

4   through the fibronectin receptor induces collagenase and stromelysin gene expression, J

5   Cell Biol 109 (1989) 877-889.

6 [35] B. Geiger, J.P. Spatz, A.D. Bershadsky, Environmental sensing through focal adhesions,

7   Nat Rev Mol Cell Biol 10 (2009) 21-33.

8 [36] N.O. Deakin, C.E. Turner, Paxillin comes of age, J Cell Sci 121 (2008) 2435-2444.

9 [37] A. Mammoto, T. Mammoto, M. Kanapathipillai, C. Wing Yung, E. Jiang, A. Jiang, K.

10   Lofgren, E.P. Gee, D.E. Ingber, Control of lung vascular permeability and

11   endotoxin-induced pulmonary oedema by changes in extracellular matrix mechanics,

12   Nat Commun 4 (2013) 1759.

13 [38] K.R. Levental, H. Yu, L. Kass, J.N. Lakins, M. Egeblad, J.T. Erler, S.F. Fong, K. Csiszar,

14   A. Giaccia, W. Weninger, M. Yamauchi, D.L. Gasser, V.M. Weaver, Matrix crosslinking

15   forces tumor progression by enhancing integrin signaling, Cell 139 (2009) 891-906.

16 [39] C.C. Lin, C.T. Kuo, C.Y. Cheng, C.Y. Wu, C.W. Lee, H.L. Hsieh, I.T. Lee, C.M. Yang,

17   IL-1 beta promotes A549 cell migration via MAPKs/AP-1- and NF-kappaB-dependent

18   matrix metalloproteinase-9 expression, Cell Signal 21 (2009) 1652-1662.

1 [40] S. Dupont, L. Morsut, M. Aragona, E. Enzo, S. Giulitti, M. Cordenonsi, F. Zanconato, J.

2   Le Digabel, M. Forcato, S. Bicciato, N. Elvassore, S. Piccolo, Role of YAP/TAZ in

3   mechanotransduction, Nature 474 (2011) 179-183.

4 [41] R.I. Fernando, M.D. Castillo, M. Litzinger, D.H. Hamilton, C. Palena, IL-8 signaling

5   plays a critical role in the epithelial-mesenchymal transition of human carcinoma cells,

6   Cancer Res 71 (2011) 5296-5306.

7 [42] M.J. Paszek, N. Zahir, K.R. Johnson, J.N. Lakins, G.I. Rozenberg, A. Gefen, C.A.

8   Reinhart-King, S.S. Margulies, M. Dembo, D. Boettiger, D.A. Hammer, V.M. Weaver,

9   Tensional homeostasis and the malignant phenotype, Cancer Cell 8 (2005) 241-254.

10 [43] A.C. Bharti, B.B. Aggarwal, Nuclear factor-kappa B and cancer: its role in prevention

11   and therapy, Biochem Pharmacol 64 (2002) 883-888.

12

13

14

1 **Figure legends**

2 Fig. 1. Stiff substrates induced temporary activation of NF-κB. (A) Immunofluorescent images

3 of nucleus (NLS-venus) and NF-κB (p65) in H-NLS cells on a stiff substrate (>1 Gpa, a cover

4 glass coated with collagen) and on a soft substrate (0.6 kPa, a collagen gel) 2 h after seeding.

5 (B) The proportion of NF-κB localization in the nucleus in H-NLS cells 0.5, 2, 4, 6 h after

6 seeding evaluated by immunofluorescent intensity. *; $P < 0.05$. Error bar = SE. n = at least 30

7 cells. (C) NF-κB activity detected by luciferase reporter assay of H1299 cells on a stiff substrate

8 (30.1 kPa, polyacrylamide gel containing 0.16% BIS) and on a soft substrate (2.0 kPa,

9 polyacrylamide gel containing 0.01% BIS) 6 h after seeding. *; $P < 0.05$. Error bar = SE. n = 3

10 independent experiments.

11

1   Fig. 2. Stiff substrates induced the temporary nuclear localization of NF-κB (p65-EGFP) in

2   living cells. (A) p65-EGFP images of H1299-p65-1 cells 2.5 h after seeding and (B) time-course

3   changes of NF-κB intensity in the nucleus of H1299-p65-1 cells 0–5 h after seeding on a stiff

4   substrate (>1 Gpa, a cover glass coated with collagen) and on a soft substrate (0.6 kPa, a

5   collagen gel). Error Bar = SE. n = 3 independent experiments.

6

1   Fig. 3. Stiff substrates induced the expression of inflammatory genes via NF-κB activation. (A)

2   Inflammatory genes and GAPDH mRNA expression detected by RT-PCR in H1299 cells on a

3   stiff substrate (>1 GPa, a plastic dish coated with collagen) or on a soft substrate (0.6 kPa, a

4   collagen gel) 6 h after seeding. (B) The relative expression of the inflammatory genes/GAPDH

5   ratio evaluated from RT-PCR (A). *; P < 0.05. Error bar = SE. n = 3 independent experiments.

6   (C) Inflammatory genes and GAPDH mRNA expressions detected by RT-PCR in H-NLS (NLS)

7   cells and H1299-p65-2 (p65-2) cells on a soft substrate (0.6 kPa, a collagen gel) 6 h after

8   seeding. H1299-p65-2 exhibited higher NF-κB activity than H-NLS did. (D) The relative

9   expression of the inflammatory genes/GAPDH ratio evaluated from RT-PCR (C). *; P < 0.05.

10   Error bar = SE. n = 3 independent experiments.

11

1   Fig. 4. Stiff substrates induced NF-κB activation via actomyosin contractions. (A) The NF-κB

2   activity in H1299 cells on a stiff substrate (>1 GPa, a plastic dish coated with collagen) and on a

3   soft substrate (0.6 kPa, a collagen gel) 6 h after seeding. NT, non-treated; Y, 10 μM Y27632 as

4   ROCK inhibitor; Bleb, 100 μM blebbistatin as myosin II inhibitor; LPA, 20 μM LPA as Rho

5   activator; DMSO, negative control for blebbistatin and LPA. *; $P < 0.05$. Error bar = SE. n = 5

6   independent experiments. (B) F-actin and di-phosphorylated MRLC (PP-MRLC)

7   immunofluorescent images of H1299 cells 45 min after seeding on a stiff substrate (>1 GPa, a

8   cover glass coated with collagen) and on a soft substrate (0.6 kPa, a collagen gel).

9   Cross-sectional views of XZ and YZ directions are shown together. The dotted line shows the

10   surface of the collagen gel. Bar = 10 μm. (C) The relative fluorescent intensity of

11   PP-MRLC/F-actin ratio evaluated from immunofluorescence images (B). *; $P < 0.05$. Error bar

12   = SE. n = at least 10 cells. (D) The protein expression of PP-MRLC, mono-phosphorylated

13   MRLC (P-MRLC), total MRLC (MRLC), and GAPDH in H1299 cells grown on a stiff

14   substrate (30.1 kPa, a polyacrylamide gel containing 0.16% BIS) and on a soft substrate (2.0

15   kPa, a polyacrylamide gel containing 0.01% BIS) 45 min after seeding. (E) The relative

16   expression of the proteins/GAPDH ratio evaluated from western blotting (D). *; $P < 0.05$. Error

17   bar = SE. n = 3 independent experiments.

18

1   Fig. 5. Stiff substrates induced spreading cellular morphology via NF-κB activation. (A)

2   Phase-contrast images of H1299 cells 24 h after seeding. (B) The cell adhesion area of H1299

3   cells 0.5, 1.5, 3.0, 12, and 20 h after seeding on a stiff substrate (>1 GPa, a plastic dish coated

4   with collagen) and on a soft substrate (0.6 kPa, a collagen gel). *; $P < 0.05$, Error bar = SE. n =

5   at least 10 cells. (C) Phase-contrast (Phase) and fluorescent images of DsRed and p65DN cells

6   on a stiff substrate (>1 GPa, a plastic dish coated with collagen) 24 h after seeding. DsRed,

7   H1299 cells transfected with DsRed backbone; p65DN, H1299 cells transfected with DsRed

8   conjugated with p65 dominant-negative mutant. (D) The cell area on a stiff substrate (>1 GPa, a

9   plastic dish coated with collagen) 24 h after seeding. *; $P < 0.05$, Error bar = SE. n = at least 20

10   cells. (E) Phase-contrast (Phase) and fluorescent images of NLS-venus in H-NLS or p65-EGFP

11   (p65) in H1299-p65-2 cells 24 h after seeding on a soft substrate (0.6 kPa, a collagen gel). (F)

12   The cell area of H-NLS (NLS), H1299-p65-1 (p65-1), and p65-2 (p65-2) 24 h after seeding on a

13   soft substrate (0.6 kPa, a collagen gel). *; $P < 0.05$, Error bar = SE. n = at least 52 cells.

14

1 **<u>Supplementary data</u>**

2 Fig. S1. Substrate stiffness between 13.8 and 30.1 kPa is critical to the activation of NF-κB in

3 H1299 cells. NF-κB activity detected by luciferase reporter assay in H1299 cells on substrates

4 of different stiffness (2.0, 13.8, 30.1, and 67.2 kPa) 6 h after seeding. Error bar = SE. n = 3

5 samples.

6

1   Fig. S2. H1299-p65-1 and H1299-p65-2 cells exhibited higher NF-κB activity than H1299. (A)

2   NF-κB activity of H1299 (WT), H1299-p65-1 (p65-1), and H1299-p65-2 (p65-2) cells on a stiff

3   substrate (>1 GPa, a plastic dish coated with collagen) 6 h after seeding, detected by luciferase

4   reporter assay. n = 3 samples. Error bar = SE. (B) NF-κB activity of H-NLS cells (NLS) and

5   H1299-p65-2 cells on a soft substrate (0.6 kPa, a collagen gel) 6 h after seeding, detected by

6   luciferase reporter assay. n = 3 independent experiments. Error bar = SE.

7

1   Fig. S3. Substrate stiffness did not affect protein expression of NF-κB. NF-κB (p65) and

2   GAPDH protein expressions of H1299 cells 2, 4, 6 h after seeding on a stiff substrate (30.1 kPa,

3   a polyacrylamide gel containing 0.16% BIS) or on a soft substrate (2.0 kPa, a polyacrylamide

4   gel containing 0.01% BIS) as detected by western blotting.

5

1   Fig. S4. Integrin β1 and ECM molecules did not affect NF-κB activation. (A) The

2   phase-contrast images of H1299 cells on a stiff substrate (>1 GPa, a collagen-coated plastic

3   dish) non-treated or treated with 400 ng/mL monoclonal antibody AIIB2, which inhibited

4   integrin β1 activity, 6 h after seeding. (B) The cell area of H1299 cells on a stiff substrate (>1

5   GPa, a plastic dish coated with collagen) 6 h after seeding. Error bar = SE. n = at least 34 cells.

6   (C) NF-κB activity of non-treated or AIIB2-treated H1299 cells on a stiff substrate (>1 GPa, a

7   plastic 24-well plate coated with collagen) 6 h after seeding, as detected by luciferase reporter

8   assay. n = 3 independent experiments. (D) NF-κB activity of H1299 cells on a plastic 24-well

9   plate coated with ECMs 6 h after seeding, as detected by luciferase reporter assay. PLL,

10   poly-L-lysine as non ECM condition; FN, fibronectin; Lam, laminin; Col, collagen. n = 3

11   samples. Error bar = SE.

12

1   Fig. S5. Y27632 treatment reduced di-phosphorylated myosin regulatory right chain

2   (PP-MRLC) whereas LPA treatment increased PP-MRLC. The protein expressions of

3   PP-MRLC and GAPDH in H1299 cells grown on a stiff substrate (>1 GPa, a plastic dish coated

4   with collagen) compared with a soft substrate (0.6 kPa, a collagen gel) 6 h after seeding. NT,

5   non-treated; Y, 10 μM Y27632 as ROCK inhibitor; LPA, 20 μM LPA as Rho activator; DMSO,

6   negative control for LPA.

1   Fig. S6. NF-κB activity did not increase di-phosphorylated myosin regulatory light chain

2   (PP-MRLC). (A) F-actin, p65-EGFP, and PP-MRLC fluorescent images of H1299 and

3   H1299-p65-2 (p65-2) cells 24 h after seeding on a stiff substrate (>1 GPa, a cover glass coated

4   with collagen) or on a soft substrate (0.6 kPa, a collagen gel). Cross-sectional views of XZ and

5   YZ directions are shown together. Bar = 20 μm. (B) Protein expression of PP-MRLC and

6   GAPDH in H-NLS (NLS) and H1299-p65-2 cells grown on a stiff substrate (30.1 kPa, a

7   polyacrylamide gel containing 0.16% BIS) and on a soft substrate (2.0 kPa, a polyacrylamide

8   gel containing 0.01% BIS) 24 h after seeding, detected by western blotting.

9

1 Fig. S7. Stiff substrates induce spread cellular morphology via NF-κB activation. (A, B)

2 Representative phase-contrast images of H1299 cells 24 h after seeding on stiff (>1 GPa, a

3 plastic dish coated with collagen) and soft (0.6 kPa, a collagen gel) substrates. (C, D)

4 Representative phase-contrast (Phase) and fluorescent images of DsRed and p65DN cells on a

5 stiff substrate (>1 GPa, a plastic dish coated with collagen) 24 h after seeding. DsRed, H1299

6 cells transfected with DsRed backbone; p65DN, H1299 cells transfected with DsRed conjugated

7 with p65 dominant-negative mutant. (E, F, G) Representative phase-contrast (Phase) and

8 fluorescent images of NLS-venus in H-NLS (E) or p65-EGFP (p65) in H1299-p65-1 (F) and

9 H1299-p65-2 (G) cells 24 h after seeding on a soft substrate (0.6 kPa, a collagen gel).

1   Fig. S8. Stiff polyacrylamide gel substrates induced spreading cellular morphology. Stiff (30.1

2   kPa), polyacrylamide gels containing 0.16% BIS; Soft (2.0 kPa), polyacrylamide gels

3   containing 0.01% BIS. (A) The phase-contrast images of H1299 cells on stiff and soft substrates

4   12 h after seeding. Bar = 100 μm. (B) The cell area on stiff and soft polyacrylamide gels 2, 4, 6,

5   12, and 24 h after seeding. Error bar = SE. n = at least 16 cells at each time of observation.

6

7

1   Fig. S9. H1299 cells transfected with p65 dominant-negative plasmid (p65DN) exhibited

2   decreased NF-κB activity. The NF-κB activity of H1299 cells transfected with or without

3   p65DN detected by luciferase reporter assay. Cells were seeded on a stiff substrate (>1 GPa, a

4   plastic 24-well plate coated with collagen) and harvested 6 h after seeding. n = 3 samples. Error

5   bar = SE.

6

1   Fig. S10. TNFα induced NF-κB activation in H1299 cells grown on a soft substrate (0.6 kPa, a

2   collagen gel). (A) The immunofluorescence images of H1299 cells treated with 15 ng/mL TNFα

3   or of non-treated (NT) H1299 cells 1.5 h after seeding in a serum-free medium. Bar = 20 μm.

4   (B) The proportion of NF-κB localization in the nucleus evaluated from intensity of

5   immunofluorescence images. n = 10 cells. Error bar = SE. (C) NF-κB activity measured by

6   luciferase reporter assay in H1299 cells 6 h after seeding. n = 3 samples. Error bar = SE. (D)

7   The immunofluorescence images of H1299 cells treated with TNFα and DMSO

8   (TNFα+DMSO) or cells treated with TNFα and 1 μM BAY-11-7082 (TNFα+BAY) 1.5 h after

9   seeding in a serum-free medium. Bar = 20 μm. (E) The proportion of NF-κB localization in the

10   nucleus was evaluated from the intensity of immunofluorescence images. n = at least 9 cells.

11   Error bar = SE.

12

1   Fig. S11. TNFα treatment induced spreading morphology in H1299 cells grown on a soft

2   substrate (0.6 kPa, a collagen gel). (A) The phase-contrast images and (B) areas of H1299 cells

3   treated with 15 ng/mL TNFα or non-treated (NT) 24 h after seeding in a serum-free medium.

4   Bar = 100 μm. n = at least 130 cells. Error bar = SE. (C) Area of H1299 cells treated with TNFα

5   and DMSO (TNFα+DMSO) or treated with TNFα and 1 μM BAY-11-7982 (TNFα+BAY) 24 h

6   after seeding in a serum-free medium. n = at least 214 cells. Error bar = SE.

7

1   Fig. S12. TNFα treatment did not increase di-phosphorylated myosin regulatory light chain

2   (PP-MRLC). (A) F-actin and PP-MRLC fluorescent images of H1299 cells non-treated or

3   treated with 15 ng/mL TNFα 24 h after seeding on a soft substrate (0.6 kPa, a collagen gel).

4   Cross-sectional views of XZ and YZ directions are shown together. Bar = 20 μm. (B) Protein

5   expression of PP-MRLC and GAPDH in H-NLS (NLS) cells grown on a stiff substrate (30.1

6   kPa, a polyacrylamide gel containing 0.16% BIS) and H1299 cells non-treated (NT) or treated

7   with 15 ng/mL TNFα grown on a soft substrate (2.0 kPa, a polyacrylamide gel containing

8   0.01% BIS) 24 h after seeding, detected by western blotting. Non-treated or TNFα-treated

9   H1299 cells were cultured with serum-free media.

10

1 Fig. S13. NF-κB activity increased adhesion ability in H1299 cells. The relative number of

2 adhering cells in H-NLS (NLS) and H1299-p65-2 (p65-2) on a stiff substrate (>1 GPa, a plastic

3 dish coated with collagen) and on a soft substrate (0.6 kPa, a collagen gel) 30 min after seeding.

4 *; $P < 0.05$, Error bar = SE. n = 3 samples.

5

1   Fig. S14. Substrate stiffness regulated the formation of focal adhesions via actomyosin

2   contractions. (A) F-actin and paxillin immunofluorescence images of H1299 cells 24 h after

3   seeding on a stiff substrate (>1 GPa, a cover glass coated with collagen) or on a soft substrate

4   (0.6 kPa, a collagen gel). White arrows indicate the adhesion sites (focal adhesions) observed as

5   paxillin dots. Cross-sectional views of XZ and YZ directions are shown together. Bar = 20 μm.

6   NT, non-treated; Y, 10 μM Y27632 as ROCK inhibitor; Bleb, 100 μM blebbistatin as myosin II

7   inhibitor; LPA, 20 μM LPA as Rho activator; DMSO, negative control for blebbistatin and LPA.

8   (B) The relative number of adhesion sites (focal adhesions) evaluated from immunofluorescence

9   images (A). *; $P < 0.05$. Error bar = SE. n = 10 cells. (C) The cell area evaluated from F-actin

10 images in immunofluorescence staining (A). *; $P < 0.05$. Error bar = SE. n = 10 cells.

11

1   Fig. S15. NF-κB activity did not regulate the formation of focal adhesions. (A) p65-EGFP and

2   paxillin immunofluorescence images of H1299-p65-2 (p65-2) cells 24 h after seeding on a stiff

3   substrate (>1 GPa, a cover glass coated with collagen) or on a soft substrate (0.6 kPa, a collagen

4   gel). White arrows indicate the adhesion sites (focal adhesions) observed as paxillin dots.

5   Cross-sectional views of XZ and YZ directions are shown together. Bar = 20 μm. (B) The

6   relative number of the adhesion sites (focal adhesions) evaluated from immunofluorescence

7   images (A). *; $P < 0.05$. Error bar = SE. n = 10 cells.

8

9

1   Video S1. Time-lapse observations of H1299-p65-1 cells on a stiff substrate (a glass coated with

2   collagen) after seeding. Cross-sectional views of XZ (horizontal) and YZ (vertical) directions

3   (axes) are shown together. Green: p65-EGFP, Video time 1 second = real time 60 min, Bar = 20

4   μm.

5

1   Video S2. Time-lapse observations of H1299-p65-1 cells on a soft substrate (a collagen gel)

2   after seeding. Cross-sectional views of XZ (horizontal) and YZ (vertical) directions (axes) are

3   shown together. Green: p65-EGFP, Video time 1 second = real time 60 min, Bar = 20 μm.

4

1

2   **Figure 1**

(A)

>1 GPa

2.5 h

0.6 kPa

2.5 h

p65-EGFP 50 µm

(B)

1

2   **Figure 2**

1

2 **Figure 3**

1

2 **Figure 4**

1
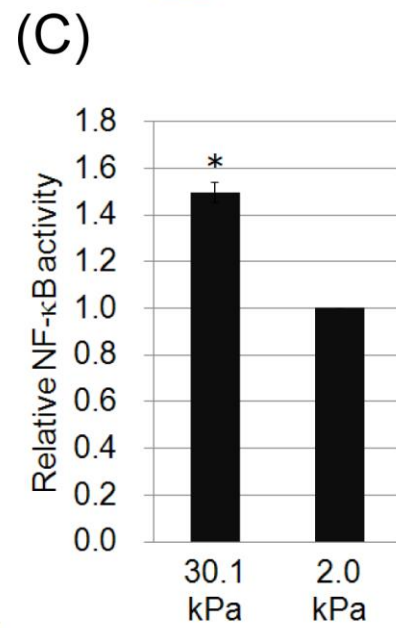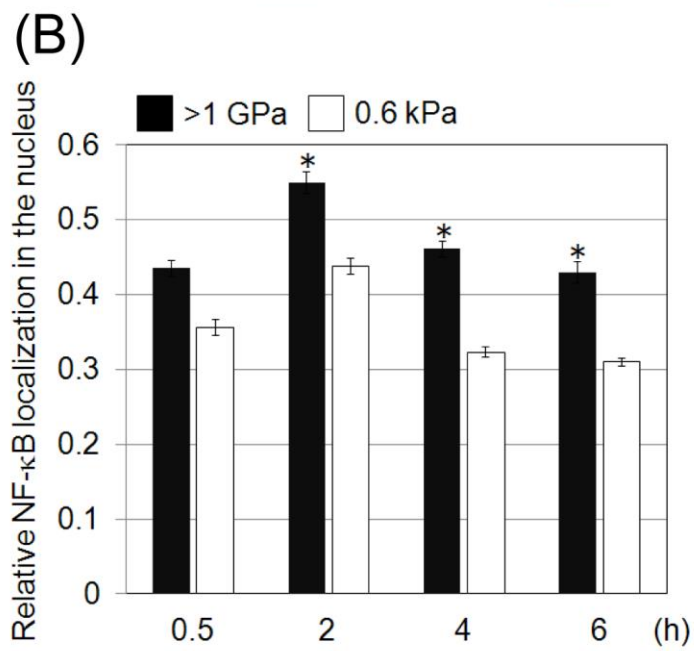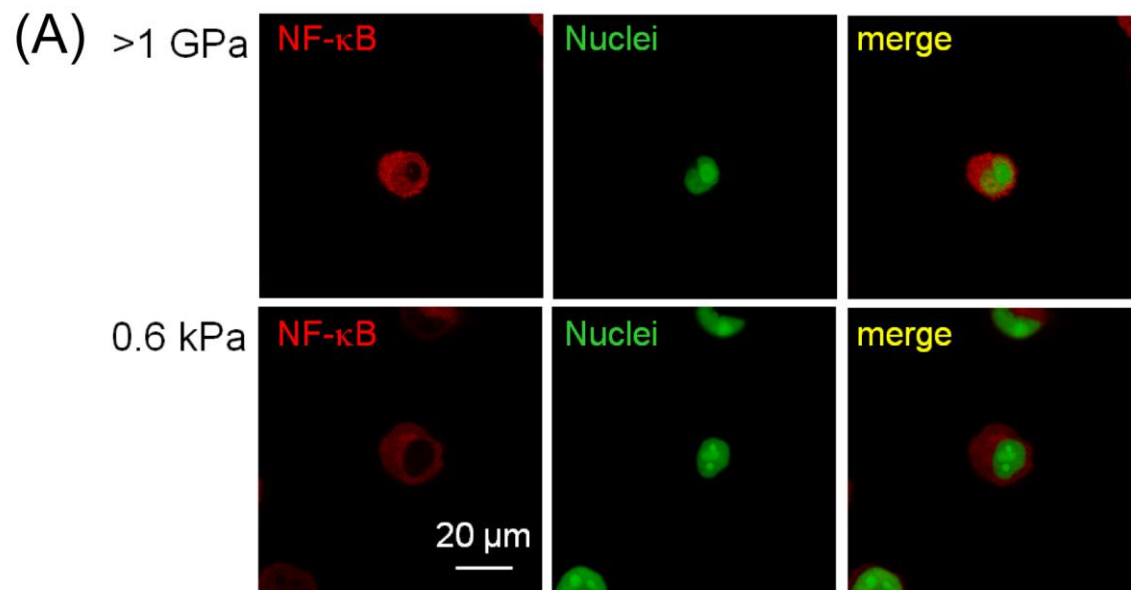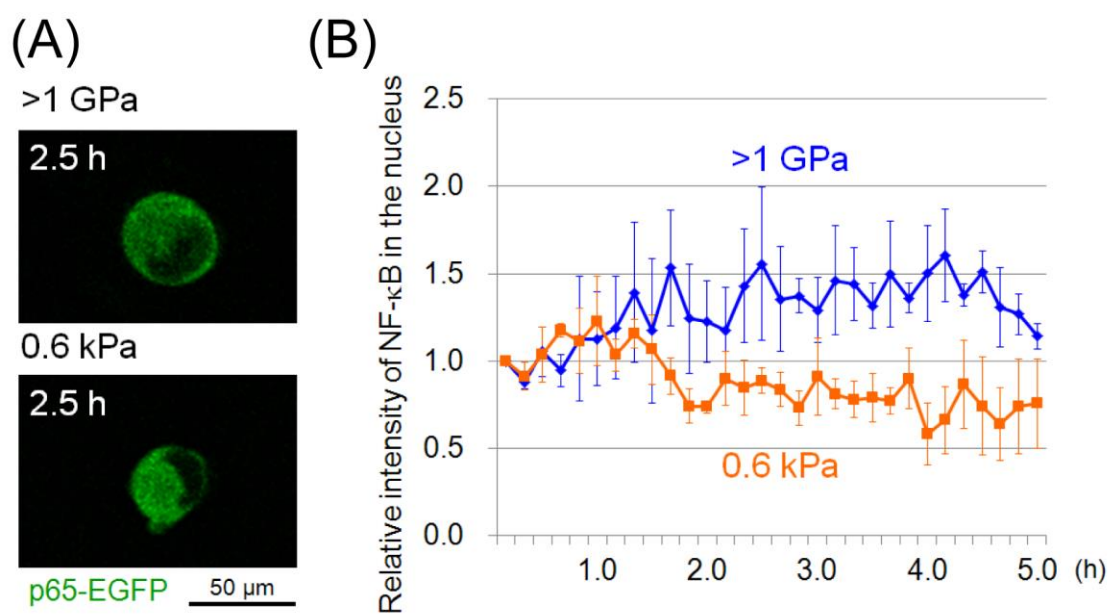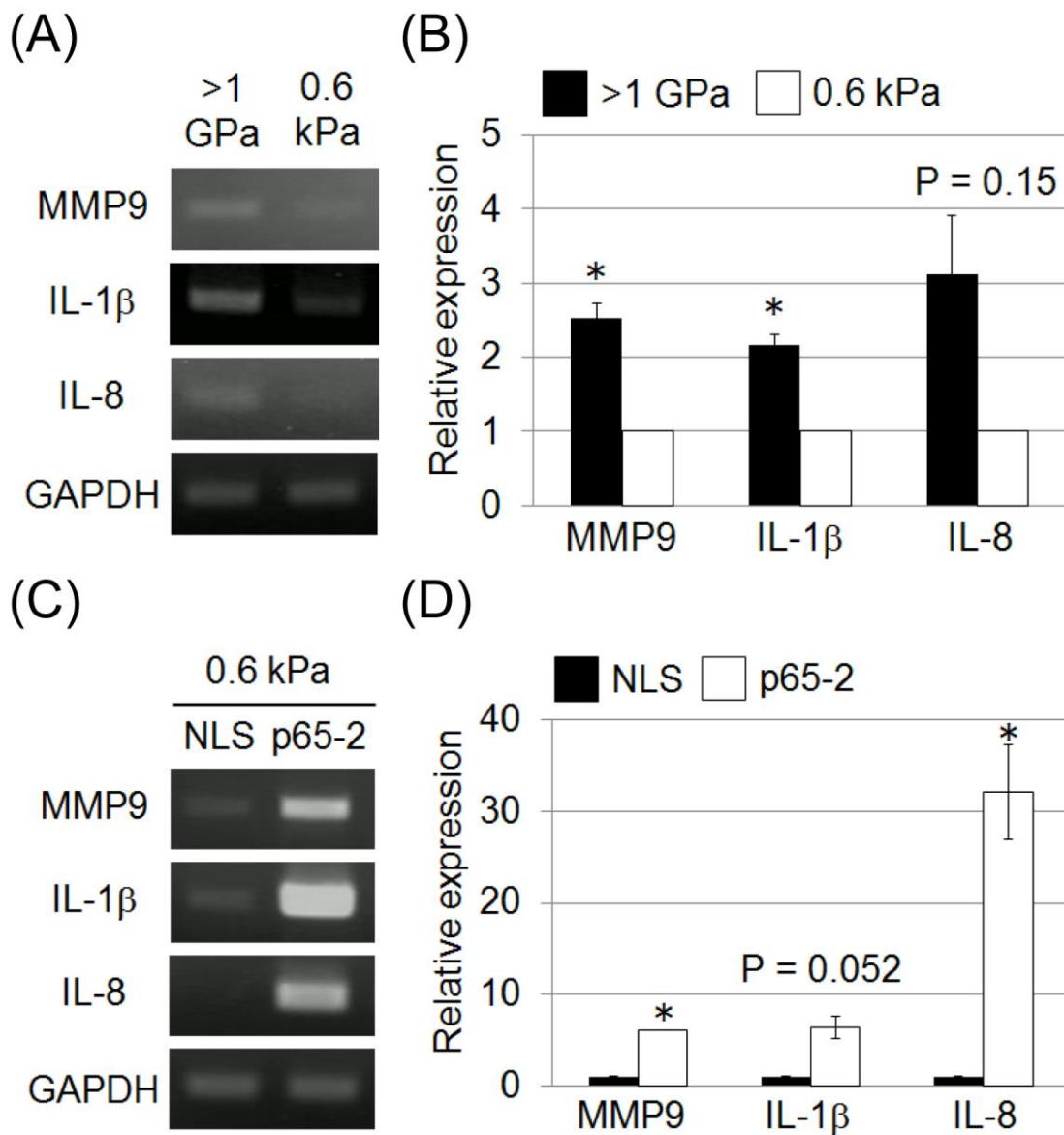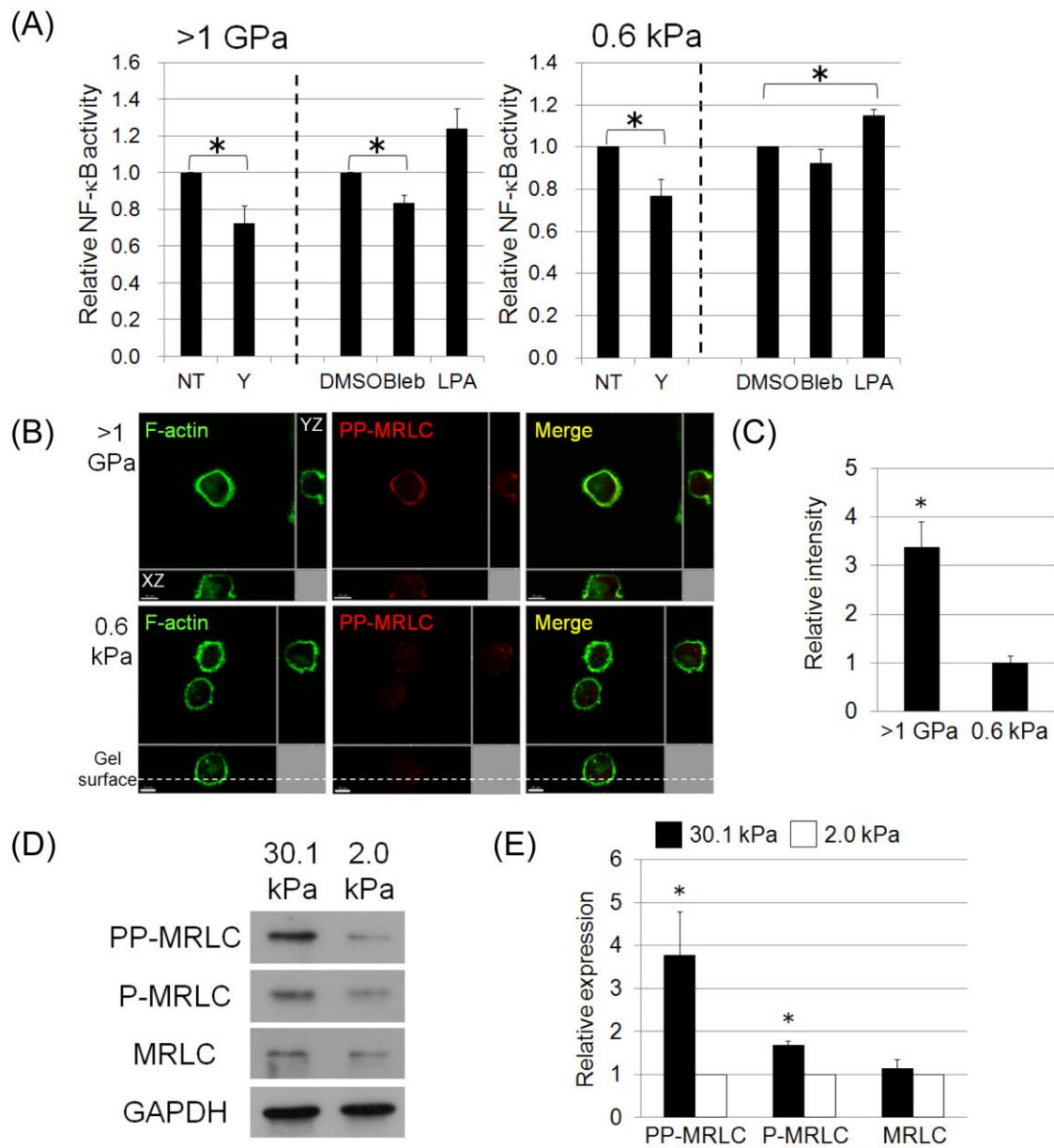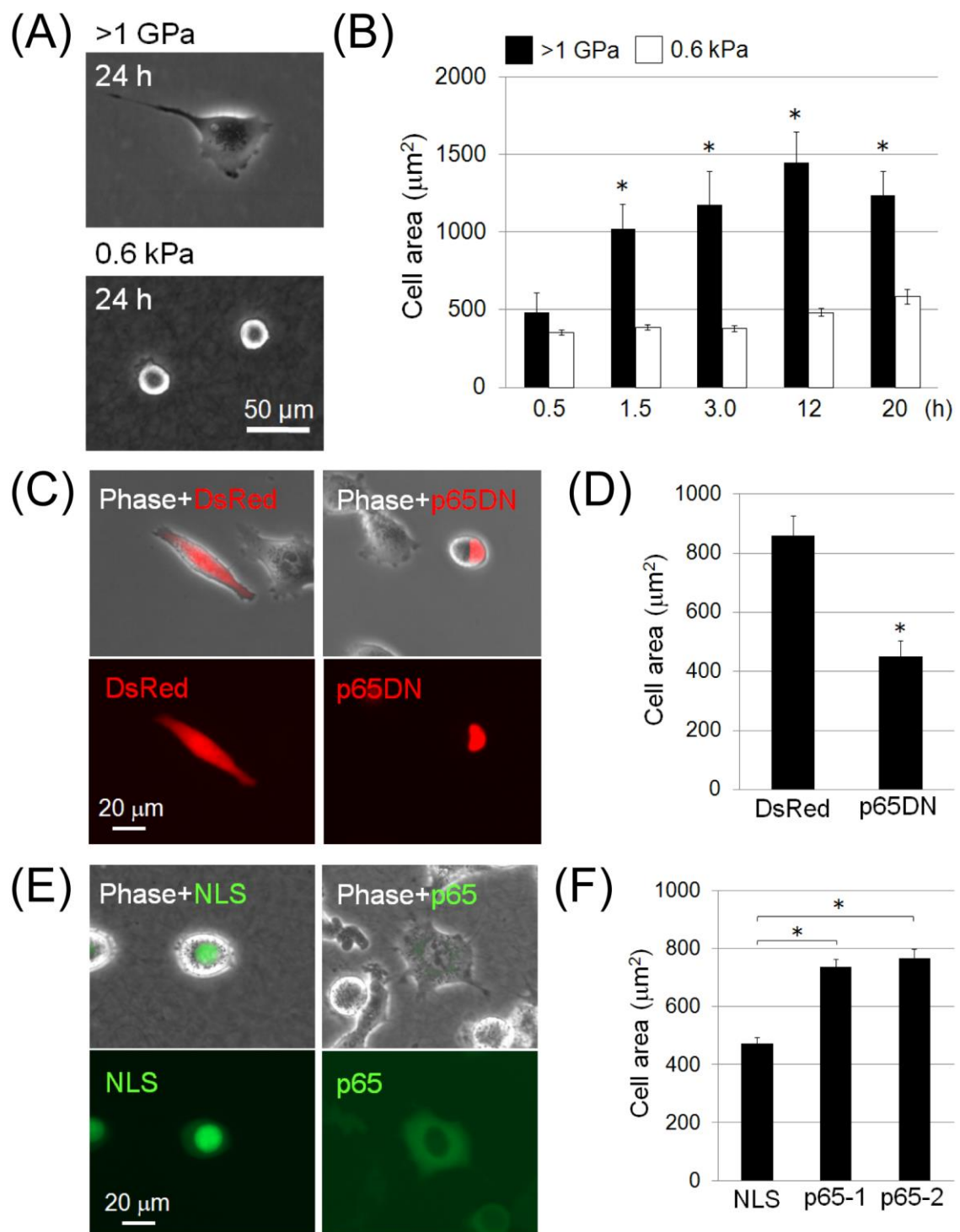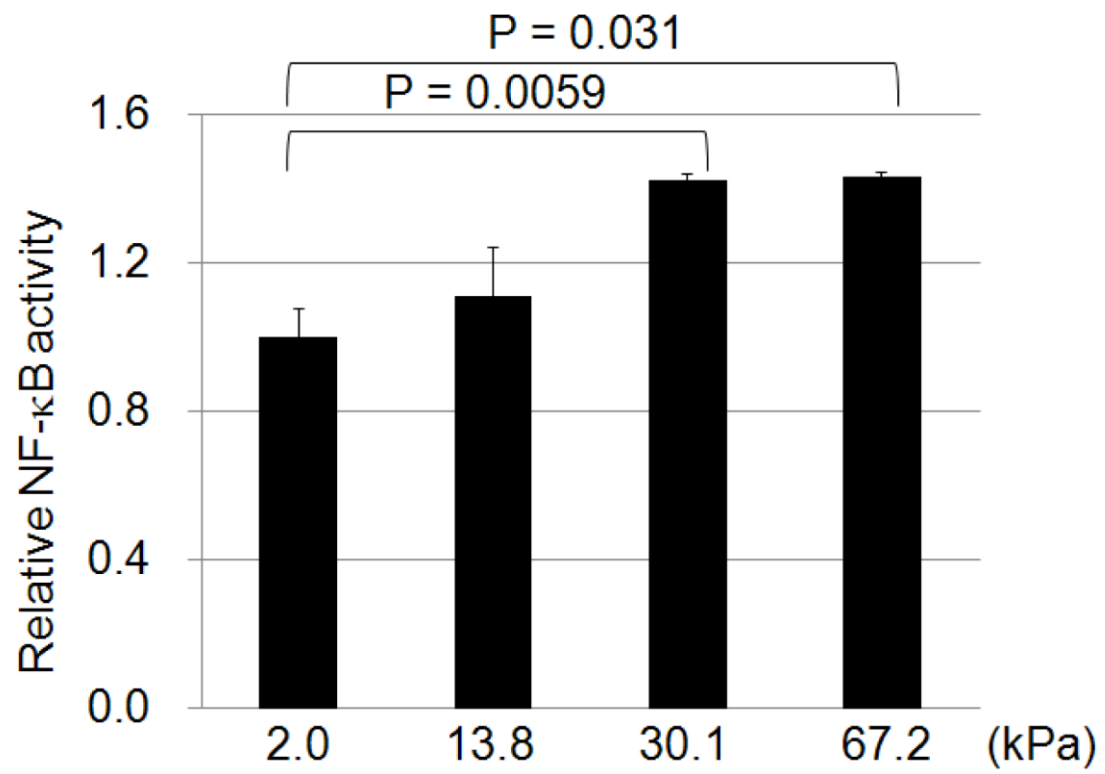
2 **Figure 5**

1

2 **Figure S1**

(A)

(B)

1

2 **Figure S2**

1

2   **Figure S3**

1

2 **Figure S4**

1

2   **Figure S5**

(A)

>1 GPa

0.6 kPa

H1299 F-actin PP-MRLC merge F-actin PP-MRLC merge

p65-2 p65-EGFP F-actin marge p65-EGFP F-actin merge

p65-EGFP PP-MRLC marge p65-EGFP PP-MRLC merge

(B)

30.1 kPa 2.0 kPa

NLS p65-2 NLS p65-2

PP-MRLC

GAPDH

1
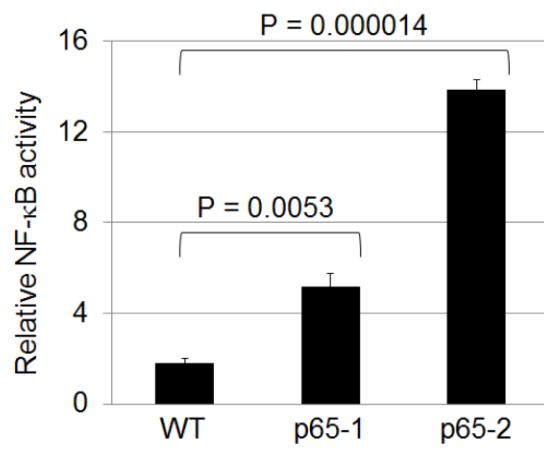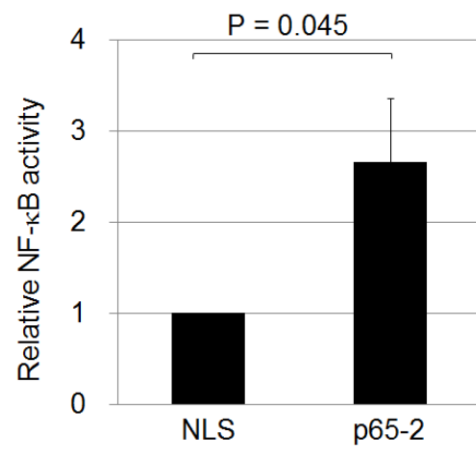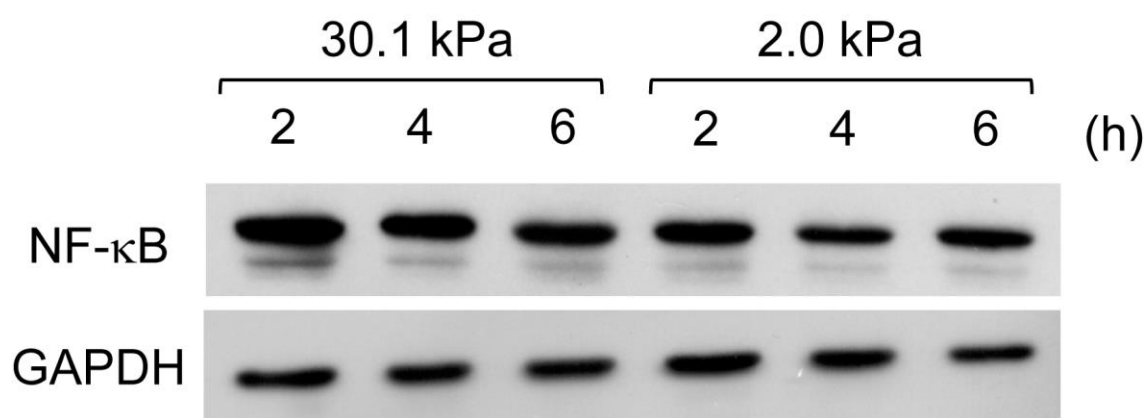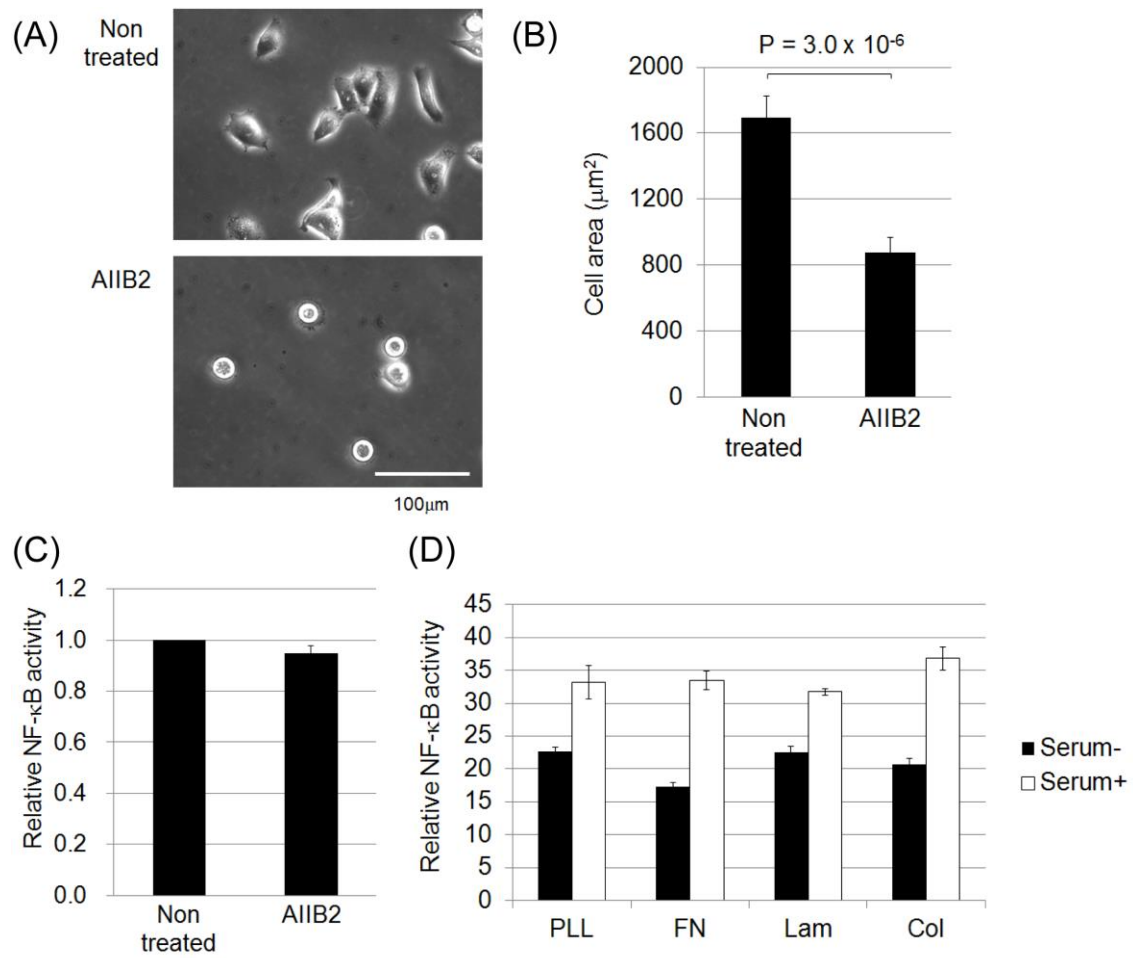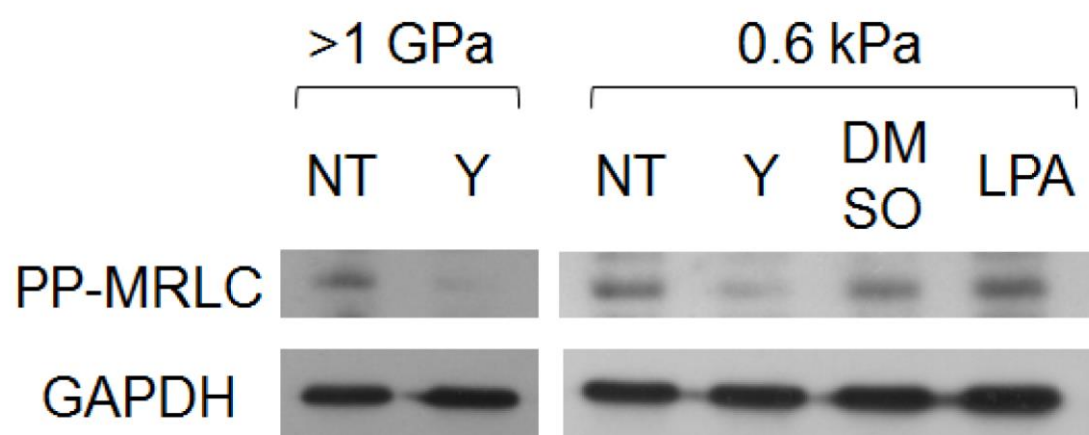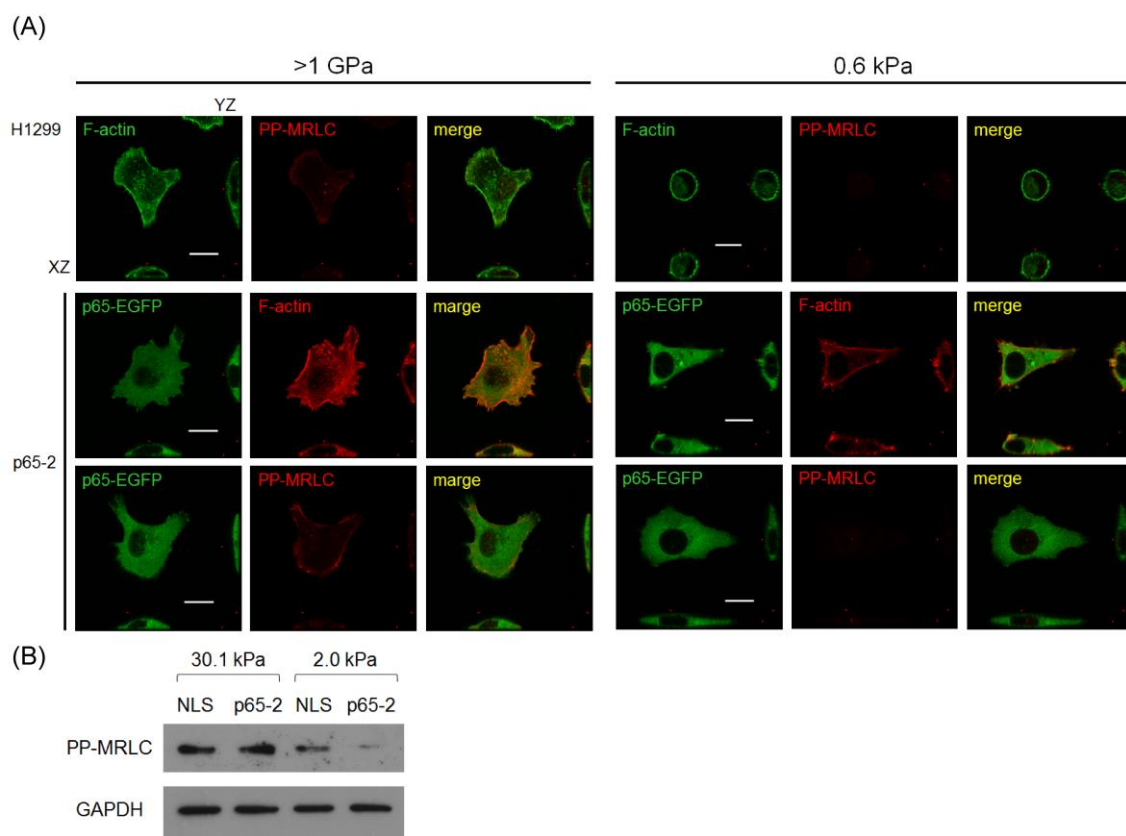
2 **Figure S6**

1

2   **Figure S7**

(A)

30.1 kPa

2.0 kPa

(B)

1

2 **Figure S8**

1

2   **Figure S9**

1

2   **Figure S10**

(A) Non treated / TNFα

(B) P = 2.1 x 10⁻¹¹

(C) P = 4.4 x 10⁻¹⁰

1

2 **Figure S11**

(A)

	F-actin	YZ	PP-MRLC	marge
Non treated				
XZ				
TNFα				

(B)

	30.1 kPa	2.0 kPa	
	NLS	NT	TNFα
PP-MRLC			
GAPDH			

1

2 **Figure S12**

Figure S13

(A)

(B)

(C)

1

Figure S14

1

2   **Figure S15**